Physical Modeling and Analysis of Rain and Clouds by Anisotropic Scaling Multiplicative Processes

DANIEL SCHERTZER[1] AND SHAUN LOVEJOY

Physics Department, McGill University, Montreal, Quebec, Canada

We argue that the basic properties of rain and cloud fields (particularly their scaling and intermittency) are best understood in terms of coupled (anisotropic and scaling) cascade processes. We show how such cascades provide a framework not only for theoretically and empirically investigating these fields, but also for constructing physically based stochastic models. This physical basis is provided by cascade scaling and intermittency, which is of broadly the same sort as that specified by the dynamical (nonlinear, partial differential) equations. Theoretically, we clarify the links between the divergence of high-order statistical moments, the multiple scaling and dimensions of the fields, and the multiplicative and anisotropic nature of the cascade processes themselves. We show how such fields can be modeled by fractional integration of the product of appropriate powers of conserved but highly intermittent fluxes. We also empirically test these ideas by exploiting high-resolution radar rain reflectivities. The divergence of moments is established by direct use of probability distributions, whereas the multiple scaling and dimensions required the development of new empirical techniques. The first of these estimates the "trace moments" of rain reflectivities, which are used to determine a moment-dependent exponent governing the variation of the various statistical moments with scale. This exponent function in turn is used to estimate the dimension function of the moments. A second technique called "functional box counting," is a generalization of a method first developed for investigating strange sets and permits the direct evaluation of another dimension function, this time associated with the increasingly intense regions. We further show how the different intensities are related to singularities of different orders in the field. This technique provides the basis for another new technique, called "elliptical dimensional sampling," which permits the elliptical dimension rain (describing its stratification) to be directly estimated: it yields $d_{el} = 2.22 \pm 0.07$, which is less than that of an isotropic rain field ($d_{el} = 3$), but significantly greater than that of a completely flat (stratified) two-dimensional field ($d_{el} = 2$).

1. INTRODUCTION

In theoretical terms the rain field can be considered to be the solution of a complex set of coupled nonlinear partial differential equations. These equations must clearly include the effect of the dynamical interactions of water vapor and liquid, latent heat release, radiation, wind fields, etc.. Structures in these fields are nonlinearly coupled over a range of over roughly 9 orders of magnitude in scale along the horizontal (~1 mm to ~1000 km), and they are therefore way beyond the scope of direct deterministic numerical modeling. In order to function at all, global models of either climate or weather rely extensively on ad hoc "subgrid scale parameterizations." These parameterizations are unsatisfactory, not only because of their unphysical nature, but also because the theoretical (mathematical) properties of the parameterized equations are fundamentally different from the original (unparameterized) ones.

For rain and cloud fields, attractive stochastic alternatives to deterministic modeling have been developed (for relevant surveys see *Waymire and Gupta* [1981], *Lovejoy and Schertzer* [1986a]). For the rain field a particularly promising approach has been to exploit its scaling properties, which relate the small- and large-scale statistical structures in a fairly simple manner [e.g., *Lovejoy and Schertzer* 1985a; *Waymire* 1985]. By simulating rain by the scaling sum of a large number of random increments or "pulses" of different sizes, one is able to produce cloud and rain field simulations that include texture, clustering, and bands as well as intermittency.

Unfortunately, the linear structure of such processes is in sharp contrast with the actual nonlinear dynamics. In distinction to these additive processes, the phenomenological cascade models studied in turbulence (reviewed in section 3) are multiplicative: the large structures multiplicatively modulate the various fluxes (e.g., of energy) at smaller scales. Additive and multiplicative scaling processes are now known to be fundamentally different [*Schertzer and Lovejoy* 1985a]. In the former case, called "simple scaling," "scaling of the increments," or "scaling in probability distributions" (see, for example *Lovejoy* [1981] or *Lovejoy and Mandelbrot* [1985]), a single scaling exponent suffices to describe the behavior of the statistical moments at different scales. In contrast, the latter case requires multiple exponents (e.g., the mean and variance etc., called "multiple scaling", scale differently) and is therefore more general. If we define structures in the field by those regions that exceed a fixed threshold, then additive processes have a single fractal dimension (independent of the threshold), while multiplicative processes have multiple fractal dimensions that decrease as the threshold is increased [*Schertzer and Lovejoy* 1983a, b, 1984, 1985a, 1986a, 1987; *Frisch and Parisi*, 1985; *Halsey et al.* 1986; *Pietronero and Siebesma*, 1986]. In simulating rain a basic choice must therefore be made between additive and

[1]Now at Etablissement d'Études et Recherches Météorologiques, Centre de Recherches en Météorologie Dynamique, Météorologie Nationale, Paris, France.

monodimensional or multiplicative and multidimensional models.

In a recent paper exploring anisotropic additive rain models [*Lovejoy and Schertzer*, 1985a], it was argued that realistic rain models should be multidimensional, if only because monodimensionality is so special: theoretically, when modeling rain, there is no a priori reason to restrict the range of dimensions to a single value. Empirical evidence that rain does indeed involve multiple dimensions was given by *Lovejoy et al.*.[1987] by using a new data analysis technique called "functional box counting."

Perhaps the most compelling reason of all to study cascades is that they are physically based: i.e., there is a direct conceptual link between the dynamical equations and the (phenomenological) stochastic model. In comparison, existing (additive) models are almost purely ad hoc in this respect. Even the simplest ("passive scalar") model of turbulent clouds, in which the cloud concentration is modified only by advection by the velocity field, is already highly nonlinear.

This paper has the dual purpose of aiming at a fair degree of rigor while at the same time remaining accessible to the wide audience of rainfall modelers who are often unfamiliar with turbulence ideas. The structure of the paper reflects this dichotomy by giving only the principle results in the main body of the text, with the derivations and more detailed discussion in the appendices. In section 2 we introduce the basic notions of scaling and cascades as well as the distinction between "dressed" and "bare" quantities. Sections 3, 4, and 5 provide an outline of multiplicative processes and how they can be used to model passive scalar cloud and rain fields. Starting from turbulent phenomenology (in sections 3 and 4), we analyze various implications (such as the divergence of moments) which arise from the singular nature of the limit of such processes, while in section 5 we give explicit methods for stochastic modeling of fluxes in continuous cascades.

These theoretical sections introduce a formalism which is not necessary in the analysis of the more familiar additive processes but which is needed here to deal with the mathematical complexity of the multiplicative processes. This complexity is best understood by making a fundamental distinction between the "bare" and "dressed" properties of the cascade [*Schertzer and Lovejoy*, 1987]. The "bare" properties are those theoretically obtained after a finite number of cascade steps, while the "dressed" quantities are the experimentally accessible averages of completed cascades (e.g., the spatial and/or temporal averages of the flux densities). In contrast, (nonpathological) additive processes do not involve similar mathematical problems; when the effects of smaller and smaller scales are included, the limit down to infinitely small sizes is simply a (random) function or measure.

The difference between the bare and dressed quantities is profound: for example, with the help of "trace moments" (section 4) we show that the multiple scaling of the bare moments implies the divergence of high-order dressed moments. Since the observables are best approximated by dressed quantities, their high-order statistical moments will generally diverge (this phenomenon is associated with the strong intermittency). Empirically, it implies the existence of "outliers," even in very large experimental samples.

The last section of the paper is devoted to the testing of our theory with high-quality radar rain reflectivities from the McGill weather radar observatory. Reflectivities are ideal for our purpose because they nonperturbatively sample the rain reflectivity field, with low instrumental noise, while providing data over a wide range of space and time scales.

When the divergence of moments is investigated, using standard probability distributions, we find $Pr(Z'>Z) \sim Z^{-\alpha}$, with $\alpha \sim 1.06$ for the probability Pr of a random reflectivity Z' exceeding a fixed Z. Moments $<Z^h>$ for $h \geq \alpha$ therefore diverge. We also empirically estimate the "trace moments" of rain (introduced in section 5), which allows us to estimate the dimension function determined by the various moments. This shows that statistical (ensemble) averages of rain depend not only on the scale, but also on the dimension over which they are averaged.

2. ELEMENTS OF SCALING AND TURBULENT CASCADES

2.1. *Simple Scaling*

In physically based rain models, as a first step, it is natural both to ignore the effect of the rain processes on the dynamics and to consider only the dynamical advection processes. This passive scalar "approximation," has the advantage of being based upon well-defined (and studied) equations (see Appendix A) and phenomenology. It is already sufficiently complex to require us to come to grips with some of the basic aspects of the nonlinear variability of clouds. Indeed, it is worth noting that in numerical weather prediction models, passive advection of water substance is the only dynamical process used to produce rain; other processes are highly "parameterized." Furthermore, as we argue in section 5, adding in other non-linear effects may not fundamentally change the cascade-type behavior of the system. If this is true, then most of the results below, as well as the basic modeling techniques will still apply.

In Appendix A we show that the dynamical equations governing passive scalar clouds involve ranges of scale within which the system has no characteristic size. In such (sub) ranges the large and small scales are related by a scale-changing operation that involves only the scale ratio: the system is said to be scaling. If the scale-changing operation is a simple magnification (zoom), then the system is statistically isotropic and is usually said to be self-similar. When the scale-changing operation is not of this particularly special and simple form, the scaling is anisotropic and is typically characterized by (fractional) differential stratification and/or rotation, although far more general transformations are possible. Even though it is clear that the atmosphere requires anisotropic scaling because of gravity and the Coriolis force, we will limit the following discussion to the simpler isotropic case (see, however, Appendix D for generalizations to anisotropy, including the modeling of stratification and the Coriolis force).

Even within the framework of isotropic scaling, many different relationships between the various scales are possible. In this subsection we review some basic turbulence phenomenology and show how it can be interpreted in terms of the scaling of probability distributions. This type of scaling involves only one parameter, hence in order to distinguish it from the more general case involving an infinite number of parameters (a function), we call it "simple

scaling." It is also called scaling of the increments and is primarily of interest when the increments rather than the process itself are stationary. Simple scaling was found empirically over limited time scales in storm-integrated rain [*Lovejoy* 1981] and was used as the basis of the scaling rain model discussed by *Lovejoy and Mandelbrot* [1985].

Consider the passive advection of water (concentration ρ) by a velocity field v in the limit of vanishing viscosity and diffusivity. As indicated in Appendix A, the nonlinear terms in the dynamical equations conserve the flux of energy and of scalar variance (with respective densities ε and χ) while effecting a transfer to smaller scales (hence the cascade). If the injection of these quantities at large scale is constant (or at least a stationary random process), the simplest assumption (going back to *Kolmogorov* [1941]) is

$$\varepsilon = -\partial <v^2>/\partial t = \text{constant}$$
$$\chi = -\partial <\rho^2>/\partial t = \text{constant} \tag{1}$$

In this interpretation ε and χ are considered spatial averages over the whole flow (these are denoted by boldface characters to distinguish them from the local quantities used later). We ignore local variability (which as we see, actually turns out to be extreme) and consider that a statistically stationary, relatively homogeneous field of these quantities exists. Then, by dimensional arguments (or by analysis of the scaling properties of the corresponding equations, see Appendix A), we are led to the celebrated scaling laws of *Kolmogorov* [1941], *Obukhov* [1949], and *Corrsin* [1951]

$$E_v(k) \approx \varepsilon^{2/3} k^{-5/3}$$
$$E_\rho(k) \approx \varphi^{2/3} k^{-5/3} \tag{2}$$

where $\varphi = \chi^{3/2} \varepsilon^{-1/2}$, and $E_v(k)$ and $E_\rho(k)$ are the power spectra for the velocity and passive scalar fields, respectively, and k is a wave number ($k=1/l$). Here φ is the flux resulting from the nonlinear interactions of the velocity and water. These formulae have corresponding expressions in real space

$$\Delta v(l) \approx \varepsilon^{1/3} l^{1/3}$$
$$\Delta \rho(l) \approx \varphi^{1/3} l^{1/3} \tag{3}$$

where $\Delta v(l)$ and $\Delta \rho(l)$ are the characteristic "fluctuations" of the fields v and ρ at the scale l (for example, the standard deviations of the differences, or increments in v and ρ at points separated by distance l). These formulae show that v and ρ are scaling, since the power law dependence on l does not involve a characteristic length. Note that since ε and φ are considered to be stationary, and they are statistically related to the increments (Δv, $\Delta \rho$), it is the latter that are stationary, rather than v and ρ themselves. If there were no factor $l^{1/3}$, then v and ρ could be obtained directly from ε and φ by regular integration; to take into account the additional scaling $l^{1/3}$, fractional integration is required. In Fourier space this is easily accomplished by multiplying by an appropriate power law filter (see section 5 and Appendix C).

If we now wish to directly relate the random fluctuations in these quantities at small-scale l, and large-scale λl, the simplest way is to suppose the following simple scaling

$$\Delta v(\lambda l) \overset{d}{=} \lambda^H \Delta v(l)$$
$$\Delta \rho(\lambda l) \overset{d}{=} \lambda^H \Delta \rho(l) \tag{4}$$

With the single parameter $H=1/3$ and with the equality "$\overset{d}{=}$"

understood as equality in probabilty distributions (hence the term "scaling of probability distributions"). However, even when there is multiple scaling (see following discussion), the tails of the probability distributions may still obey (4): see, for example, *Schertzer and Lovejoy* [1985b] (vertical wind shears, log potential temperatures) and *Lovejoy and Schertzer* [1986b] (climatological temperatures).

It is worth noting that the assumption of nonsingular behavior for ε and χ directly leads to singular behavior for the velocity and scalar fields: $H=1/3$ means that this latter are at most "one-third differentiable" ($C^{1/3}$), since, for example $\Delta v(l) \sim l^{1/3}$, hence, $\partial v/\partial x \sim \Delta v/l \sim l^{-2/3}$ which diverges as l tends to 0 [see *Richardson*, 1926; *Leray*, 1934; *Von Neumann*, 1963].

Furthermore, in this case the scaling spectra ($E_v(k)$, $E_\rho(k)$) can be exactly derived in, for example the nonlinear stochastic model produced by the renormalization procedures ("spectral closures") detailed by *Herring et al.* [1982]. These renormalization techniques can be extended to more complex situations, such as those involving interactions with the radiation field [*Schertzer and Simonin*, 1982].

2.2. Intermittency and Multiple Scaling: Bare and Dressed Quantities

The scaling indicated in (3) would presumably hold if the quantities ε and χ are not too inhomogeneous or singular, i.e., when they may be approximated by their spatial (three-dimensional) averages (see appendix A). For example, the physically significant quantity ε is not a large-scale spatially averaged quantity but a local (time and space) energy-flux density; the rate of energy flowing through an elementary volume. Its spatial (volume) average is often referred to as the energy dissipation rate. This may be considered either as a real dissipation at the smallest (viscous) scale or, rather, as an apparent dissipation at larger scales. Physically it is simply the (density of the) rate of energy transferred to smaller scales. The same comments hold for the passive scalar variance flux χ.

Early on, *Landau and Lifshitz* [1963] questioned the regularity of the density ε, since, at least in the atmosphere, it is doubtful that the external forces acting on large scales are homogeneous. Clearly, if ε and χ themselves exhibit singular behavior then this will modify the singularities of the velocity and passive scalar fields.

In order to study the question of homogeneity of ε and χ, we will use cascade processes which, by iterating a scale invariant step, systematically reduce the scale of homogeneity to zero. We write ε_l, χ_l to indicate that the largest scale of homogeneity is l (see illustration, Figure 1). These intermediate (theoretical) quantities (the "bare" quantities, see following discussion) will be seen to be highly variable (intermittent) but nevertheless (in accord with equation (3)), scale invariant. In general, we may expect that the various statistical moments of ε_l and χ_l to show the following type of "multiple" scaling (reflecting the scale invariant interactions of the fluxes)

$$<\varepsilon_l^h> \sim l^{-(h-1)C(h)}$$
$$<\chi_l^h> \sim l^{-(h-1)C'(h)} \tag{5}$$

where $C(h)$ and $C'(h)$ are decreasing functions, which are shown later to be codimensions (i.e., differences between the
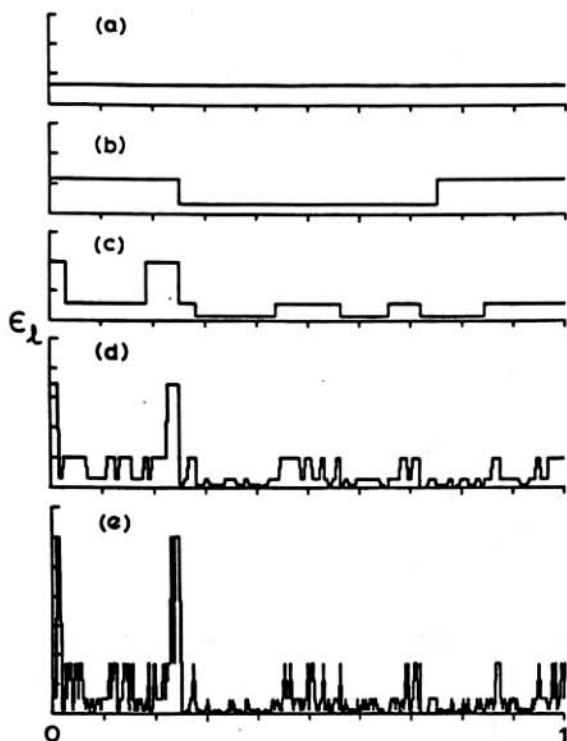
Fig. 1. We show a function which starts of homogeneous (constant) over the entire interval shown in Figure 1a, whose scale of homogeneity is then sytematically reduced by a successive factors of 4 in Figure 1b,1c,1d, and 1e. This is an example of a cascade "α-model" (section 3), parameters $C=0.4$, $\alpha=2/3$, which has the property of (on average) conserving the area under the curve (representing the energy flux to smaller scales). Because of this constraint the increasingly high peaks must become more and more sparse. The limit of the function when the scale of homogeneity goiesto zero, ts dominated by singularities distributed over sparse fractal sets.

dimensions of the space and the process). Note that the factor $(h-1)$ implies that $<\varepsilon_l>$ and $<\chi_l>$ are stationary (independent of l), as required. By comparing quantities "homogenized" over decreasing scales l (rather than increments over the same distance), it is possible to directly define the scaling (and indeed multiple scaling) of these (stationary) quantities. The nonstationary fields v and ρ are still related to ε and φ by (3), (i.e., with the additional scaling $l^{1/3}$, again requiring a fractional integration), although now (4) only holds approximately. For the present time it is sufficient to note that the nonlinear dependence on h (through the functions $C(h)$, $C'(h)$) corresponds to the multiple scaling and expresses the fact that generally, the most intense regions will scale differently than the weak regions.

The densities ε_l define the fluxes of energy over the set A (dimension $D(A)$) with the same scale of homogeneity

$$\Pi_l(A) = \int_A \varepsilon_l \, d^{D(A)}x \qquad (6)$$

(we can similarly define the corresponding flux for χ_l). What is now of interest is the behavior of Π_l and ε_l as the scale of homogeneity tends to zero. In particular: how can we define the limits Π and ε, and in what sense do they converge? It turns out (sections 4 and 5) that the limits of the densities

are very singular and are in fact only implicitly defined by the more regular limit of the fluxes. However, even in the latter case we show that in general, given a set A, there exists a critical exponent α $[=\alpha(A)]$ such that

$$<\Pi(A)^h> = \infty \quad h \geq \alpha, D(A) < C(\alpha) \qquad (7)$$

although, in contrast, for all h,

$$<\Pi_l(A)^h> < \infty \qquad (8)$$

i.e., we obtain divergence of the high-order statistical moments of the limit flux.

This nontrivial singular limit leads us to make a clear distinction between quantities homogeneous at scale l obtained after partial construction of the cascade, (which we call "bare",) and those of a completed cascade integrated over the same scale, called "dressed" quantities. Since the observation process involves averaging over finite scale, this "dresses" the "bare" quantities. The expressions "bare" and "dressed" are renormalization jargon (usually referring to partial and completely resummed diagrams in perturbation expansions of nonlinear equations). Here we have the same distinction with respect to the different degrees of multiplication implied by the various levels of the cascade: by completion of the process (and averaging on given scale and dimension) "bare" quantities are "dressed" becoming observables.

In real cascades, viscosity always eventually homogenizes the flow at the Kolmogorov or dissipation scale η, which in the atmosphere is of the order of millimeters or less. The experimental, dressed quantities at scale $l>>\eta$ are therefore no longer truly divergent for $h\geq\alpha$; they are, however, extremely large, being of the order $\Lambda^{f(h)}$, where $f(h)$ is a positive, increasing exponent, and $\Lambda=l/\eta$ $(>>1)$. Physically, this is the exact opposite of the usual situation in which the statistical properties are determined by the large-scale processes (such as energy injection, ect.). Here it is rather the small-scale details that are all-important.

An important consequence of these singular limits is that they exclude the possibility of constructing limiting scaling processes with lognormal probabilities (as shown by *Waymire and Gupta* [1987], these probabilities are incompatible with single scaling). Indeed, partially constructed processes which are lognormal do not tend to lognormal limits as the scale of homogenization tends to zero (if only because of the divergent moments!). Thus not only are lognormals unattainable as limits of scaling processes, they will not even be particularly good approximations to the latter. As the resolution of a lognormal model is increased, not only will the lognormal parameters continuously change, but also, ultimately, no suitable parameters can be chosen at all; the best that can be hoped for is a rough approximation to the lowest-order moments (i.e., those that converge).

Empirically the critical exponents in storm-averaged rainfall are, roughly $\alpha_R \approx 5/3$ [*Lovejoy*, 1981] radar reflectivity, $\alpha_Z \approx 1$, and in the wind field, $\alpha_v \approx 5$, and $\alpha_\varepsilon \approx \alpha_v/3 \approx 5/3$ in both the atmosphere and laboratory experiments (see discussion by *Schertzer and Lovejoy* [1985a, b, c] and *Levich et al.* [1984], *Levich and Tzvetkov* [1985], and *Levich* [1987]). As pointed out elsewhere [*Schertzer and Lovejoy*, 1983a, 1984], a finite value of α gives rise to an (additional) spurious scaling very similar to
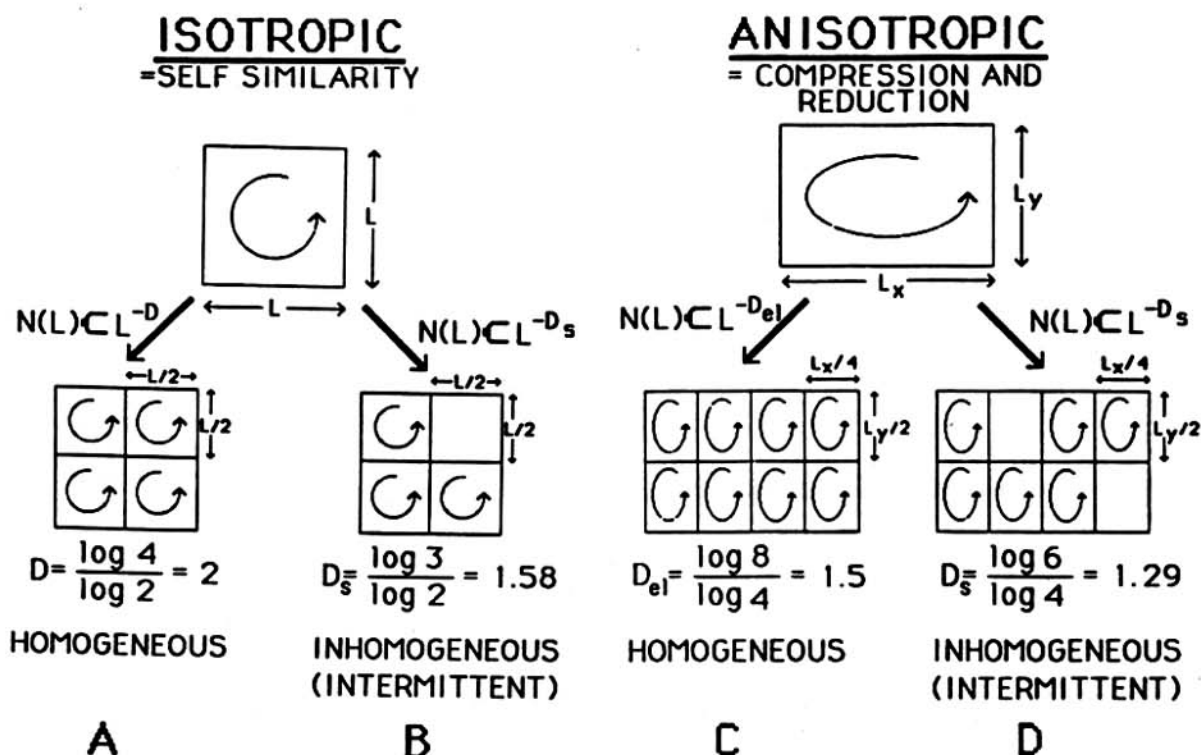
ISOTROPIC
=SELF SIMILARITY

ANISOTROPIC
= COMPRESSION AND REDUCTION

$N(L) \subset L^{-D}$ $N(L) \subset L^{-D_s}$ $N(L) \subset L^{-D_{el}}$ $N(L) \subset L^{-D_s}$

$D = \dfrac{\log 4}{\log 2} = 2$ $D_s = \dfrac{\log 3}{\log 2} = 1.58$ $D_{el} = \dfrac{\log 8}{\log 4} = 1.5$ $D_s = \dfrac{\log 6}{\log 4} = 1.29$

HOMOGENEOUS   INHOMOGENEOUS (INTERMITTENT)   HOMOGENEOUS   INHOMOGENEOUS (INTERMITTENT)

A   B   C   D

Fig. 2. (a) A schematic diagram showing one step of an isotropic homogeneous cascade. (b) Same as Figure 2a, but inhomogeneous case. (c) Same as 2a for anisotropic case (see Appendix D). (d) Same as Figure 2c but for inhomogeneous case.

that observed in the wind tunnel experiments [Anselmet et al., 1984] and further supports the value $\alpha_v \approx 5$.

2.3. Hierarchies of Singularities

It might be guessed (with certain provisos, see section 4.1) that the singular behavior of the statistics will be generated by singularities in ε of various orders $\gamma (\gamma > 0)$

$$\varepsilon_l \geq l^{-\gamma} \qquad (9)$$

(i.e., that as l tends to zero, ε_l diverges at least as fast as $l^{-\gamma}$). The (abstract) possibility of such behaviour has been hypothezised by Frisch and Parisi [1985], and by Halsey et al. [1986]. Here we show that such singularities are concretely and directly generated by cascade processes (as pointed out by Schertzer and Lovejoy [1983a,b,1985b]) and are characterized by a second (increasing) codimension function $c(\gamma)$. These and related results are important because they give us an effective means of building models with "multifractal" behavior (using the terminology of Frisch and Parisi [1985]); i.e., the structure of the process can be ascribed to an ensemble of singularities of different orders, each distributed over sets, with dimension decreasing as the order increases.

3. PHENOMENOLOGICAL CASCADES AND DISCRETE MULTIPLICATIVE PROCESSES

3.1. Phenomenology and Cascade Schemes

Ever since Richardson [1922], the phenomenology of turbulence has been described by self-similar (isotropic) cascade schemes in which an identical, scale invariant step is repeated down to the smallest scale [Novikov and Stewart, 1964; Novikov, 1965, 1966, 1967, 1969, 1970; Yaglom, 1966; Gurvitch and Yaglom, 1967; Mandelbrot, 1974]. In the following, for simplicity we discuss only the dynamical (i.e., energy flux) cascade involving a hierarchy of eddies breaking up into smaller and smaller subeddies, transfering their flux in the process, but the treatment is basically the same for passive scalar variance flux. Figure 2 gives a schematic example: a large eddy in the center is broken up (via nonlinear interactions with other eddies or through internal instabilities) into smaller subeddies, homogeneously (Figure 2a) or inhomogeneously (Figure 2b). These schemes can be dynamically interpreted as two-dimensional spatial cuts, taken at different times, of a four-dimensional space-time process and have been recently developed for studying showers of cosmic rays [Bialas and Peschanski, 1986]. In the simplest (albeit unrealistic) isotropic, homogeneous case (Figure 2a) the number N_o of offspring (subeddies) is related to the number N_g of generators (eddies) by

$$N_o = \lambda^d N_g \qquad (10)$$

with λ being the scale ratio for one step of the cascade ($\lambda = l_n/l_{n+1}$, $\lambda > 1$, l_n being the size of an eddy at the step n), and d the dimension of the space on which the cascade occurs. Anomalous or fractal dimensions appear as soon we include the effects of inhomogeneity. The simple inhomogeneity shown in Figure 2b arises when we allow subeddies to be either "dead or alive" and involves a unique dimension characterizing the support of turbulence [Mandelbrot, 1976; Frisch et al. 1978]. The "support" is the region on which the energy flux is concentrated (using the expression of Batchelor and Townshend [1949]: its "spotty"
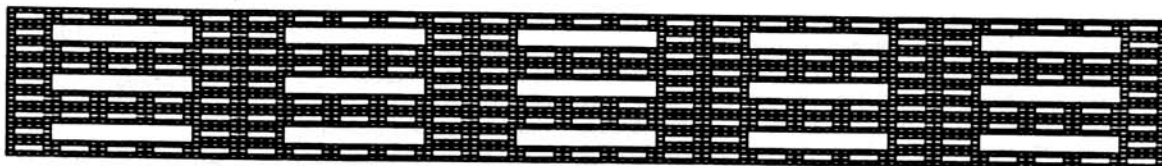
Fig. 3. An example of an anisotropic and deterministic β model with a 5 times 3 "generator" whose pattern is repeated to smaller and smaller scales with the central three rectangles inactive (white). The dimension of the active regions is therefore $D_s = \log 12/\log 5 = 1.54$ and the elliptical dimension of the whole space is $d_{el} = \log 15/\log 5 = 1.68$. The stratification, which increases at larger and larger scales, simulates that of the atmosphere (note that the rain field is considerably more stratified: the corresponding value for a vertical rain cross-section is $d_{el} = 1.22$).

regions) and has a dimension D_s given by

$$N_{o,a} = \lambda^{D_s} N_{g,a} \tag{11}$$

The subscript a indicates alive (sub) eddies.

This simple scheme, often referred to as the "β-model," yields a random Cantor set supporting the content of the activity (see Figure 3). Unfortunately, it is not stable to "small" pertubations which yield the "α-model" (see later discussion). Once we abandon the alternative "dead or alive," choosing subeddies to be either "strong" or "weak," the uniqueness of the dimension of the support is lost. Indeed, in the former case at each cascade step all the alive subeddies will be of equal strength (every one of their ancestors must be "alive"). Furthermore, in the limit $n \to \infty$, they belong to a sparse fractal set of dimension $D_s < d$, and hence in order to preserve the volume average of the density of energy, this density (the "strength" of the subeddies) must increase without bound, becoming singular. However, we are still dealing with a unique type of singularity. In the deterministic case (i.e., iterating exactly the same step), the singularity can be removed by employing the D_s-dimensional Hausdorff measure instead of the d-dimensional Lebesgue measure: the density of the energy-flux, with respect to this measure, will simply be the indicator function of the limiting fractal set (unfortunately, this is true only to within a nontrivial constant). The stochastic case follows roughly the same rule, but requires generalized Hausdorff measures (required in order to avoid logarithmic divergences: see Mauldin et al. [1986]).

The turbulence could be said to be "fractally homogeneous" [Mandelbrot, 1974]. In the case of the α-model (see Figure 4 for an illustration), the succession of weak and strong modulating factors renders the survival of eddies more complex and leads to a continuum of eddy strengths and hence to a hierarchy of singularities. Furthermore, it is obvious that the spectrum of singularities will broaden as soon as we take the hth power of ε: large h will drastically reduce the importance of the "weak" subeddies and simultaneously reinforce the strongest subeddies; conversely, small values of h will smooth out differences between subeddy strengths.

More generally, the scale invariant step is specified by the identically distributed random variables $\mu\varepsilon$, which prescribe the fraction of flux transmitted from one eddy to its offspring. It represents the collective effect of all the nonlinear interactions relevant in the breakup process, i.e., in shorthand (and self-explanatory notation)

$$\varepsilon_{subeddy} = \varepsilon_{eddy} (\mu\varepsilon) \tag{12}$$

the symbol μ is used to denote a multiplicative increment analogous to the way that the symbol Δ is used to indicate an additive increment. Note that we also have

$$\Pi_{subeddy} = \Pi_{eddy} (\mu\Pi)$$
$$\mu\Pi = \lambda^{-d} \mu\varepsilon \tag{13}$$

This is obvious, since in computing the d-dimensional fluxes

Fig. 4. An example of a (random) anisotropic α-model with $d_{el} = \log 20 /\log 5 = 1.86$, $C(1) = 0.16$, $C_\infty = 0.46$, with grey shades proportional to the log of ε.

over a subeddy and its parent the density of the flux is constant over the subeddy and eddy respectively.

In (13) the increments $\mu\Pi$ must be restricted so that the cascade obeys an appropriate conservation law (here determined by the nonlinear terms of Navier-Stokes equations, see Appendix A). As in classical thermodynamics, a distinction can be made between "microcanonical" and "canonical" conservation of energy, the former referring to detailed conservation (appropriate to a closed system), and the latter, allowing for exchange with the external world, involves only conservation of ensemble averages. Here the quantity of interest is the energy flux rather than the energy itself, hence we merely require conservation of its ensemble average (the atmosphere is considered an open system). It is worth adding other arguments for the canonical approach. In the microcanonical case [Yaglom, 1966], we require

$$\sum_{\text{subeddies}} \mu\varepsilon = \text{number of subeddies} = \lambda^d \qquad (14)$$

which prevents the $\mu\varepsilon$ at each step in the cascade from being fully independent of each other, since the sum is rigidly constrained. Mandelbrot [1974] pointed out that this distinction is of little relevance when, as in the present case, we are interested in fluxes on sparse sets where detailed conservation no longer holds anyway. In the canonical case we have

$$< \sum_{\text{subeddies}} \mu\varepsilon > = \lambda^d \qquad (15)$$

Hence $<\mu\varepsilon> = 1$. Although we no longer have strict detailed conservation, we nevertheless still obtain a "weak detailed conservation law" as a consequence of the independency of the $\mu\varepsilon$

$$<\Pi_{n+1}(A)>_n = \Pi_n(A) \qquad (16)$$

where $< >_n$ stands for the expectation conditioned by the first n steps of the cascade, $\Pi_{n+1}(A)$ and $\Pi_n(A)$ for the ($D(A)$-dimensional) fluxes over nearly any $D(A)$-dimensional set A which is not too sparse (see later discussion). This law (known in probabilistic terms as the "martingale property" [Feller, 1971]) is quite important, since it establishes the convergence properties of the process.

3.2. Discrete Cascades

In a cascade process discretized on cubes, as outlined in the previous section, the multiplicative "increments" $\mu\varepsilon_n$ are in fact "top hat" functions that are constant on cubes B_n (of size $l_n = \lambda^{-n} l_0$), the value being given by independent realizations of a positive random variable $\mu\varepsilon$. The only constraint on the probability distribution of the random variable is the conservation of flux ($<\mu\varepsilon>= 1$).

In order to be more explicit, let us (temporarily) denote the functional dependence of $\mu\varepsilon_n$ and ε_n by

$$\varepsilon_n(x) = \sum_J \varepsilon_{n,J} \, 1_{B_n,J}(x)$$

$$\mu\varepsilon_n(x) = \sum_J \mu\varepsilon_{n,J} \, 1_{B_n,J}(x)$$

$$(17)$$

where $1_{B_n,J}(x)$ is the indicator function of the cube $B_{n,J}$ and

n, J labels the different balls of size l_n; e.g., taking $l_0=1$ (the unit cube) for a given cascade step n, J is the dXn array of the first n, base-λ digits of the coordinates of the centers of $B_{n,J}$, and $\mu\varepsilon_{n,J}$ are independent realizations of the random variable $\mu\varepsilon$ (for different n, J).

As an example, consider the "α-model" introduced by Schertzer and Lovejoy [1983a, b,1985b] (see Figures 1 and 4). Its specification is

$$Pr(\mu\varepsilon = \lambda^{C/\alpha}) = \lambda^{-C}$$
$$Pr(\mu\varepsilon = \lambda^{-C\alpha'}) = 1 - \lambda^{-C} \qquad (18)$$

where the positive parameters C, α, and α' are chosen to satisfy conservation of flux ($<\mu\varepsilon>=1$), and Pr indicates probability. This reduces to the β-model for $\alpha=1$ (implying $C/\alpha'=\infty$). When $\alpha=1$, the single and oft-cited parameter is $\beta=\lambda^C$ (rather than the more natural choice C, which is the codimension ($=d-D$) of the surviving eddies in the β-model). Here the less extreme survivors have lower codimensions and hence larger dimensions. From (18) and the definition in (5), we obtain the following codimension function $C(h)$

$$C(h) = \frac{C}{\alpha}\left(1 + \frac{1-\alpha}{h-1}\right) + O\left(\frac{1}{h^2}\right) \qquad h \rightarrow \infty \qquad (19)$$

In section 4 we confirm that, as indicated in (7), that the hth moments of the energy flux, integrated over set A, diverge when $D(A)<C(h)$. Not only does this allow us to theoretically describe such a hierarchy of singularities, it also gives us a practical means to investigate it by "sensing" (averaging) these singularities with various observational sets (A). When the cascade is "sensed" by averaging it over low-dimensional A, the most intense and sparsest singularities will not be directly felt: there is not sufficient "room" on A for the integration to smooth out the strongest singularities of this set. However, as shown later, the fact that we have not reached the highest singularities still makes itself indirectly felt via the divergence of the high-order statistical moments.

3.3. Theoretical Development

To study more general cascades, it is convenient to introduce the $\log_\lambda$ of $\mu\varepsilon$, denoted γ

$$\mu\varepsilon \doteq \exp(\gamma \ln \lambda) = \lambda^\gamma \qquad (20)$$

which, as an exponential increment, plays the role of a generator satisfying the group property

$$\varepsilon_{m+n} = T_n(\varepsilon_m)\varepsilon_n \qquad (21)$$

where ε_m and ε_n are independent m and n generation cascades. $T_n(\varepsilon_m)$ simply means that the process starts not from unit cubes (of size l_0), but from cubes of size l_n; i.e., T_n is the contraction of ratio λ^{-n}. (i.e., $T_n[\varepsilon_m(x)]=\varepsilon_m(\lambda^{-n}x)$).

Without excluding the possibility of degeneracy ($\varepsilon_n(x)\rightarrow 0$, almost surely everywhere), then any (real) random variable γ can be used as a generator of a cascade process with the following (flux conserving) normalization

$$e^{\gamma'} = \frac{e^\gamma}{<e^\gamma>} \qquad (22)$$

where γ' is the corresponding normalized (flux conserving) generator, the formula for ε_n is given in terms of the corresponding functions Γ_n.

$$\varepsilon_n = \frac{e^{\Gamma_n}}{\langle e^{\Gamma_n}\rangle} \qquad \Gamma_n = \sum_{m \leq n} \gamma_m \qquad (23)$$

Where the functional dependence of Γ_n and γ_n is of the same sort as for ε_n. The multiplicative group property (21) implies that the Γ_n satisfy the additive group property

$$\Gamma_{n+m} = T_n(\Gamma_m) + \Gamma_n \qquad (24)$$

It is important to note that though the functions γ_n are independent, the hierarchical structure of the model builds up long-range dependencies through the overlapping of the support of these functions (corresponding to the relationship between subeddies having a common ancestor). Indeed, the sum over the generators γ produces the scaling law for the different moments ε_n. This is simply expressed through the second characteristic function K of γ (in base λ) defined by

$$\langle e^{h\gamma}\rangle = e^{K(h)\log\lambda} = \lambda^{K(h)} \qquad (25)$$

We now obtain the simple result

$$\langle\varepsilon_{m+n}{}^h\rangle = \lambda^{n[K(h)-hK(1)]}\langle\varepsilon_m{}^h\rangle \qquad (26)$$

($K(1)=0$ for normalized generator).

We now look in more detail at the appearance of various orders of singularities as the cascade proceeds, for concreteness, considering the α-model. We are interested in how the probabilities associated with different singularities evolve. Consider a slightly more general (multistate) α-model ($c_{i,j}$ increasing with j, for a given i)

$$Pr(\gamma=\gamma_i) = p_i \sum_{j=1; \ M(i)} q_{i,j}\lambda^{-c_{i,j}} \qquad p_i>0, \ q_{i,1}=1 \qquad (27)$$

where in the two-state α-model we have $\gamma_1=C/\alpha$ ($p_1=1$, $M(1)=1$; $C_{1,1}=C$), $\gamma_2=C/\alpha'$ ($p_2=1$, $M(2)=2$; $C_{2,1}=0$, $C_{2,2}=0$, $q_{2,1}=-1$). The $M(i)$ are called "submultiplicities" and the $C_{i,j}$ have a (rather intuitive) meaning of codimensions associated with the singularity of order γ_i (more precisely, the probability of finding the singularity γ_i decomposed over $M(i)$ d-dimensional spaces, is proportional to a measure scaling as $\lambda^{-C_{i,j}}$ over each space, see *Schertzer and Lovejoy* [1987] for more details). After n steps, the same type of decomposition still holds but becomes increasingly more complex (introducing new types of singularities $\gamma_i^{(n)}$, and corresponding codimensions $c_{i,j}^{(n)}$). However, since $K(h)$ is simply the Laplace transform of the probability, it approaches, for large λ (i.e., for a large number of steps and using the saddle point approximation), the Legendre transform of the largest exponents ($c_{i,1}$) of the probability (the multiplicity becomes irrelevant). Hence $c(\gamma)$, defined as the Legendre transform of $K(h)$, corresponds simply to the limit of $c_{i,1}^{(n)}$; i.e.,

$$\lim_{n\to\infty} c_{i,1}^{(n)} = c(\gamma) = \max_h [h\gamma - K(h)]$$
$$K(h) = \max_\gamma [h\gamma - c(\gamma)] \qquad (28)$$

The preceeding derivation holds for more general probability distributions, and indeed, *Frisch and Parisi* [1985] proceeded to a similar derivation postulating (27), without considering the submultiplicity problem. The above shows that the submultiplicity is irrelevant and that multiplicative processes directly yield the same result. The use of continuous

multiplicative processes has the further advantage of showing that the function $c(\gamma)$ need not be bounded (Appendix C). In any case (28) establishes a direct link between the order of the singularities and the order of the statistics.

4. Basic Properties of Multiplicative Processes

4.1. The Singular Nature of the Small-Scale Limit

The discrete cascade model concentrates energy flux via multiplicative increments ($\mu\varepsilon_n$) on very sparse regions of the space, while on most of the space, $\varepsilon_n(x)\to 0$. One can guess what is going on from the wildly varying functions obtained after few iterations of the process (Figure 1): most of the space becomes inactive, while the increasingly sparse active regions become infinitely active (correponding to the singularities of different orders) while conserving the total flux ($\langle\varepsilon_n\rangle=1$). In fact, for any point x, $\varepsilon_n(x)\to 0$ almost surely (this is quite different from the degenerate situation where $\varepsilon_n(x)\to 0$ almost surely everywhere). For example, in the β-model the probability of an eddy surviving goes to zero as $l_n{}^C$ (here degeneracy results when $C>d$). More generally, the probability of a point becoming a singularity of order γ goes to zero as $l_n{}^{c(\gamma)}$. This extreme sparseness of the singularities is obviously required to prevent divergence of all orders.

The limit ε of the ε_n can no longer be a density (i.e., an ordinary function in distinction to the ε_n); however, it remains an operator (as the ε_n are) that converts (linearly) one measure (the volume of given set of little cubes) into another (the energy flux on the same set). Indeed, we may anticipate that the behavior of the fluxes $\Pi_n(A)$ for any (Borel) set A will be far more regular than the ε_n. More precisely, since $\Pi_n(A)$ are positive (bounded) martingales (see the discussion on the conservation of the flux, section 3), they have for any (Borel) set A almost surely a limit (the Doob theorem, e.g., *Feller* [1971])

$$\Pi(A) = \lim_{n\to\infty} \Pi_n(A) \qquad (29)$$

thus implicitly defining the limit ε of the ε_n as a linear operator on measures. We will keep the standard notation for integration in order to make this definition more explicit

$$\int_A \varepsilon \, dm = \lim_{n\to\infty} \int_A \varepsilon_n \, dm \qquad (30)$$

for any measure m finite on a (Borel) set A (almost surely). The above limit for the ε_n is a "weak" limit, as discussed by *Kahane* [1985, 1987]. This type of convergence leads us to study how the sequence ε_n ($n\to\infty$) operates on various measures, characterizing how the energy is distributed over these different sets (e.g., planes, surfaces, sparse (fractal) sets, etc.). At the same time, on a given set A we can characterize the way the convergence occurs by studying the different moments and particularly their finiteness (in mathematical terms, the relevant L^h space).

In the following we will restrict our attention to Hausdorff measures, which are particulary well suited to characterizing sparse sets (i.e., determining their "volume"). We will show, with the help of the basic properties of these measures
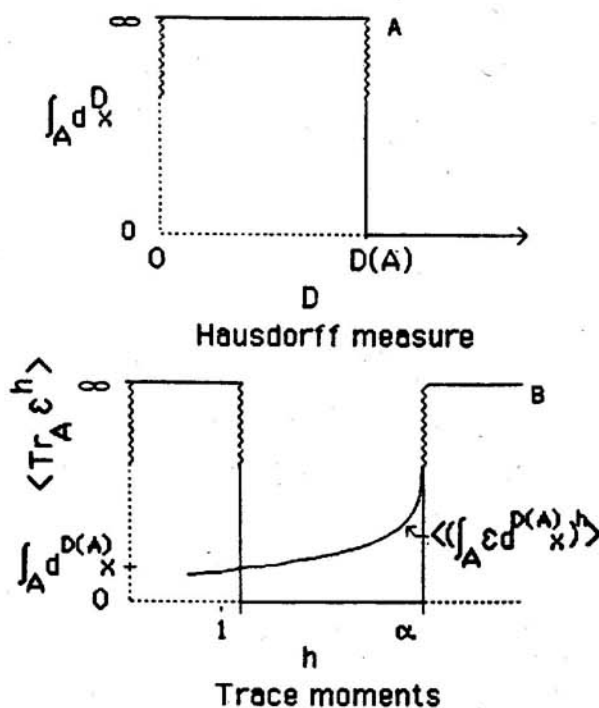
Fig. 5. (a) A schematic diagram showing the behavior of Hausdorff measures of dimension D, of the set A. Finite nonzero values (if they occur) are obtained only at the unique value $D=D(A)$. (b) A schematic illustration of the behavior of the trace moments as a function of h for a nondegenerate cascade, when the flux in a region A is integrated over a dimension $D=D(A)$. The curve represents a typical (convex) dressed flux moment, which diverges at $h=\alpha$.

(recalled in the following subsection), that the corresponding dressed moments of the flux diverge and that this is directly related to the existence of a well-defined sequence of fractal dimensions. The argument, in rough outline, is as follows: the hth order statistical moments of the D-dimensional fluxes are associated with a specific (high) dimensional Hausdorff measure. Such measures are infinite when the Hausdorff dimension is too small and zero when it is too large (see Figure 5). The divergence of moments corresponds precisely with the divergence of the corresponding Hausdorff measure when the dimension is smaller than a critical dimension.

Indeed, consider a measure defined by the hth power of ε (this is given a precise meaning later in terms of the "trace moments"). Increasing h singles out stronger and stronger singularities. The strength of these hth order singularities is then quantified by operating the measure on test (empirically, on observational) sets A of increasing dimension $D(A)$. This mathematical procedure has a direct physical counterpart: it corresponds to averaging the energy either with instruments of various dimensions (e.g., an airplane, $D(A)=1$, a satellite $D(A)=2$, or an in situ network, with $1<D(A)<2$ [Lovejoy et al. 1986a, b]).

For small enough $D(A)$ this smoothing operation is insufficient to damp out the divergences: the corresponding Hausdorff measures remain infinite. As $D(A)$ is increased above some critical value, the measure becomes zero. This transition is a basic property of Hausdorff measures. We thus obtain a direct relationship between the divergence of moments and multiple fractal dimensions. For every moment, there corresponds a critical dimension required to "tame" it.

4.2. Hausdorff Measures, Trace Moments: Degeneracy and Divergence of High-Order Statistics

In order to stress the fact the D-dimensional Hausdorff measures are generalizations of the usual volume (Lebesgue) measures, we denote them by

$$\int d^D x$$

In the cubic discretization used here,

$$\int_{B_n} d^D x = \lambda^{-D} l_0^D$$

where $l_n = \lambda^{-1} l_0$ is the size of the cubes (B_n), (or more generally of the "balls" defining the topology, see Appendix D concerning anisotropy) these measures generalize the usual fact that the length of a surface is infinite, while its volume is zero, since the Hausdorff dimension $D(A)$ of A is defined by the following divergence rule

$$\int_A d^D x = \infty \qquad D < D(A)$$
$$\int_A d^D x = 0 \qquad D > D(A) \tag{31}$$

i.e., the Hausdorff measure with $D=D(A)$ dimension is the only one (see Figure 5a) which can be finite and nonzero (a property we will assume later for the different $D(A)$-dimensional sets A). An important property of Hausdorff measures is that they have a simple scaling relation (with respect to any dilation of scale ratio λ; $A \to \lambda A$)

$$\int_{\lambda A} d^{D(A)} x = \lambda^{D(A)} \int_A d^{D(A)} x \tag{32}$$

We are interested in the (usual) moments of the flux $\Pi(A)$ defined as

$$<\Pi(A)^h> = <\left(\int_A \varepsilon d^{D(A)} x \right)^h> \tag{33}$$

for the set A.

Unfortunately, these ordinary moments are difficult to handle, since for noninteger h, they are not Hausdorff measures. To deal with the different powers of ε in a more convenient (and rigorous) fashion, we are led to a definition of the hth trace moments of the flux by first defining the trace of Π^h, over a set A, as being

$$Tr_A \Pi^h = \int_A \varepsilon^h d^{hD(A)} x \tag{34}$$

As detailed in Appendix B, the right-hand side of (34) can given a precise meaning (consistent with the notation used in equation (30)) as being the tracelike part of (33) (as can be anticipated by comparing the two right-hand sides). Note that the hth power of ε is not easy to define, since no property of martingale is directly connected to it.

The trace-moments are simply the resulting (ensemble) averages of these quantities

$$<Tr_A \Pi^h> = <\int_A \varepsilon^h d^{hD(A)} x> \tag{35}$$

Appendix B also shows that the convexity of the second characteristic function ($K(h) = (h-1)C(h)$) of the generator and the relationships between trace and usual moments lead to the twin divergence rule indicated schematically in Figure 5b.

This rule can be summarised as follows:

1. A low h divergence ($h<1$) of the trace moments is needed to avoid degeneracy of the process: $C(1)<D(A)$ ($\leq d$).

2. A large h divergence ($h>1$) results from h large enough (and/or $D(A)$ small enough) respecting $D(A)<C(h)$.

In case 2 there is a direct physical interpretation in terms of an intersection theorem described in sections 5 and 6; when A is sufficiently sparse so that $D(A)<C(h)$, then the measuring set will not in general intersect the region in which the h_{th} moment is "concentrated." In other words the corresponding order of singularities γ is rarely intersected, but gives an extreme contribution, "outliers", leading to the divergence of moments.

The latter divergence occurs (except for the β-model: $C(h)=C(1)$) for sufficiently sparse (or low-dimensional) sets A. Conversely, this divergence is removed ("smoothed-out") by integrating over sets with large enough dimension as soon as the sequence of codimension $C(h)$ is bounded by $C_\infty<d$ (the dimension of space where the cascade process takes place). In the special case of the α-model, we have the simple result $C_\infty=C$ (not necessarily less than d), and continuous multiplicative processes lead to unbounded codimension function $C(h)$. See section 6 for discussion of some relevant empirical results.

5. NUMERICAL MODELING OF CONTINUOUS CASCADES

5.1. *Bare Continuous Cascades*

The discrete cascade processes discussed in section 3 have the disadvantage that they involve ugly (and unrealistic) straight lines that are artifacts of the construction procedure and which introduce a slight departure from strict translational invariance. In the discrete case (section 3) the cascade was obtained by multiplying top hat functions with algebraically decreasing scales (logarithmic discretization). To produce continuous cascades we replace these top hats by noises whose largest scale of homogeneity ($l=l_o/\lambda$) is defined by the maximum excited wave number ($k_{max}=\lambda/l_o$). In outline (see Appendix C for a more detailed discussion) the multiplication of these noises is then effected by exponentiating the integral (sum) of the logarithm of the noises. More precisely, it is found that in order to obtain multiple scaling of the bare quantities the logarithm (Γ_λ, the continuous equivalent of the discrete Γ_n of section 3) of the (bare) flux Π_λ (defined down to scale l_o/λ), must have a spectrum $E_{\Gamma\lambda}(k)$ proportional to k^{-1} for wave numbers $1/l_o \leq k \leq \lambda/l_o$ (0, elsewhere). This assures that the autocorrelation function of Γ_λ is proportional to the logarithm of λ, hence assures multiple scaling. Keeping within the standard Gaussian framework (other "universality" classes are discussed in Appendix C) and considering a Gaussian white noise $\gamma_2(k)$ (i.e., independant Gaussian variables, zero mean, unit variance, k is the wave vector modulus) filtered by the factor $k^{-d/2}$ (i.e. a fractionnal integration) we obtain

$$\Gamma_\lambda(k) = \gamma_2(k)\, k^{-d/2}\, C_1^{1/2} \qquad 1/l_o \leq k \leq \lambda/l_o \qquad (36)$$

(0, elsewhere) where the constant of proportionality ($C_1^{1/2}$) is chosen to assure $C(1)=C_1$.

To numerically simulate such a field, it therefore suffices to (1) distribute a gaussian white noise over a discrete grid in Fourier space; (2) filter the noise with a $k^{-d/2}$ filter; (3)
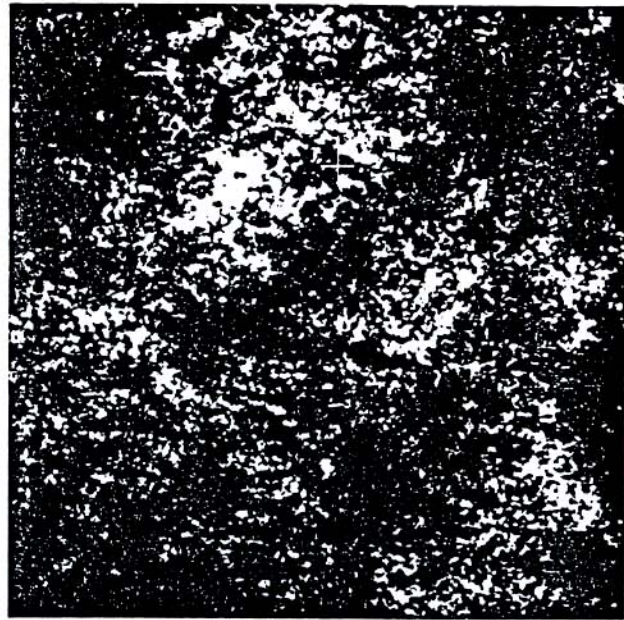

Fig. 6a. An example of multiplicative process with a Gaussian generator on a 512^2 grid. The grey scales indicate the log of ε above a threshold. Here the threshold is very low so as to display most of the singularities.

Fourier transform to yield a real space field with logarithmic correlation function; and (4) exponentiate the result to yield a continuous cascade process flux (see examples in Figure 6a and 6b). A technical point worth noting is that one must take care in order to obtain the correct normalization of the resulting field (i.e. $<\varepsilon>=1$). In particular, replacing the continuous integral by a discrete sum requires a correction (equals to the Euler constant $\gamma_e=0.57...$), since

$$\left(\int_1^n \frac{dx}{x} - \sum_{i=1}^n \frac{1}{i} \right) \to \gamma_e$$

as $n\to\infty$.

If we now wish to model a passive scalar, the simplest (though extreme) procedure is to assume that the energy and passive scalar variance fluxes (ε, χ) are completely dependent random fields, and hence φ has the same statistical properties as ε (since $\varphi = \chi^{3/2}\varepsilon^{-1/2}$). With this assumption the field produced previously can be interpreted as a field for φ (see discussion in section 2), and ρ can be simulated by adding the extra scaling $l^{1/3}$ to the field $\varphi^{1/3}$ (since $\Delta\rho(l)\approx\varphi^{1/3}l^{1/3}$). To effect this change in scaling ("fractional integration"), it suffices to (5) transform the quantity $\varphi^{1/3}$ back into Fourier space, (6) filter with the function k^{-s} with $s=H+d/2$, and (7) retransform back into real space. Since the phases have not been altered, only the spectral amplitudes, the result is a scale invariant smoothing operation, an example of which is shown in Figure 6c. The entire procedure for simulating passive scalars therefore involves three Fourier transforms, which can be efficiently performed numerically thanks to fast Fourier transform (FFT) routines. Hence even large-scale simulations are relatively inexpensive, being limited only by memory and FFT efficiency (for example, Figures 6b and c were obtained on a microcomputer). The conceptual simplicity of the model, combined with the relative ease with which it can be
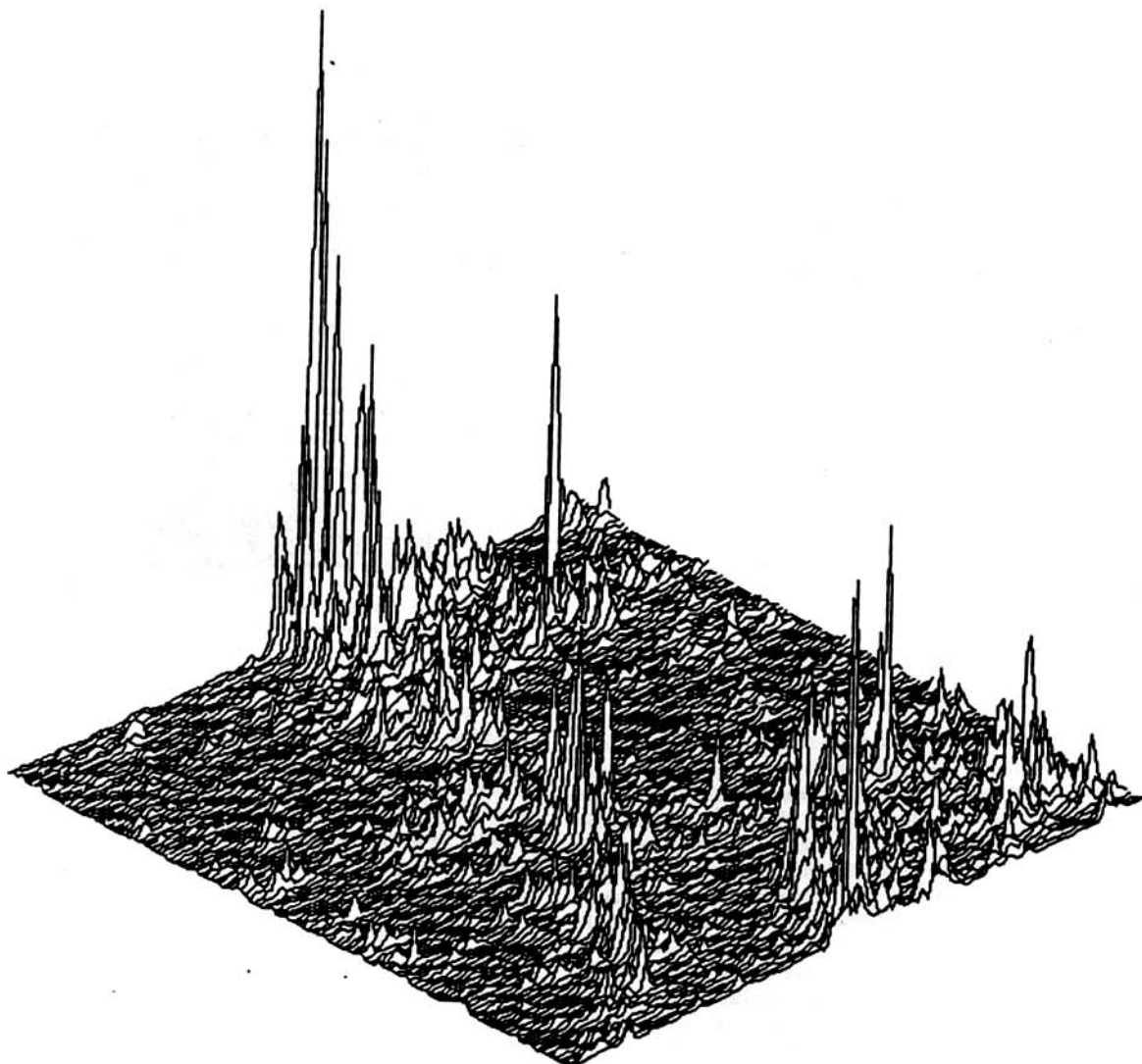
Fig.6*b*. A perspective plot of a realization of multiplicative process on a 128^2 grid clearly showing its singular nature (cf. the sharp spikes).

implemented numerically, promises to permit the future development of more sophisticated and (hopefully) realistic models (see new developments by *Wilson et al.* [1987]). An interesting next step would be to model the temporal evolution of a coupled wind/water field.

5.2. Dressed Continuous Cascades

The continuous cascade model described above simply renders the discrete case discussed in section 3 continuous; i.e., it creates a continuous, but bare, cascade. As usual, the experimentally accessible quantities are the spatially averaged, dressed ones. If we average the cascade flux itself then all the previously developed properties of dressed quantities hold (such as the divergence of moments). If instead, we average some nonlinear function of such a quantity (as a satellite might do when it averages radiances),

then the model can be used to numerically examine the effects of nonlinear averaging.

In the case of multifractal networks this can be solved by the means of a generalized intersection theorem pointed out in *Schertzer and Lovejoy* [1987]) and exploited in *Montariol and Giraud* [1986], *Margnet and Piriou* [1987] for rain measurement: the codimension-functions $C(h)$ and $C_M(h)$ of respectively the rain rate and measurements densities simply add to give the corresponding codimension-function $C_i(h)$ of the measured rain, thus generalizing the intersection theorem. Conversely, up to the critical order of divergence (see section 6.4), the codimension-function $C(h)$ of the rain rate can be estimated as $C_i(h)-C_M(h)$.

In the atmosphere the cascade breaks down at very small (but nonzero) scale η (typically of the order of millimeters) as a result of the action of viscosity. However, the theoretical dressed properties (obtained by averaging over
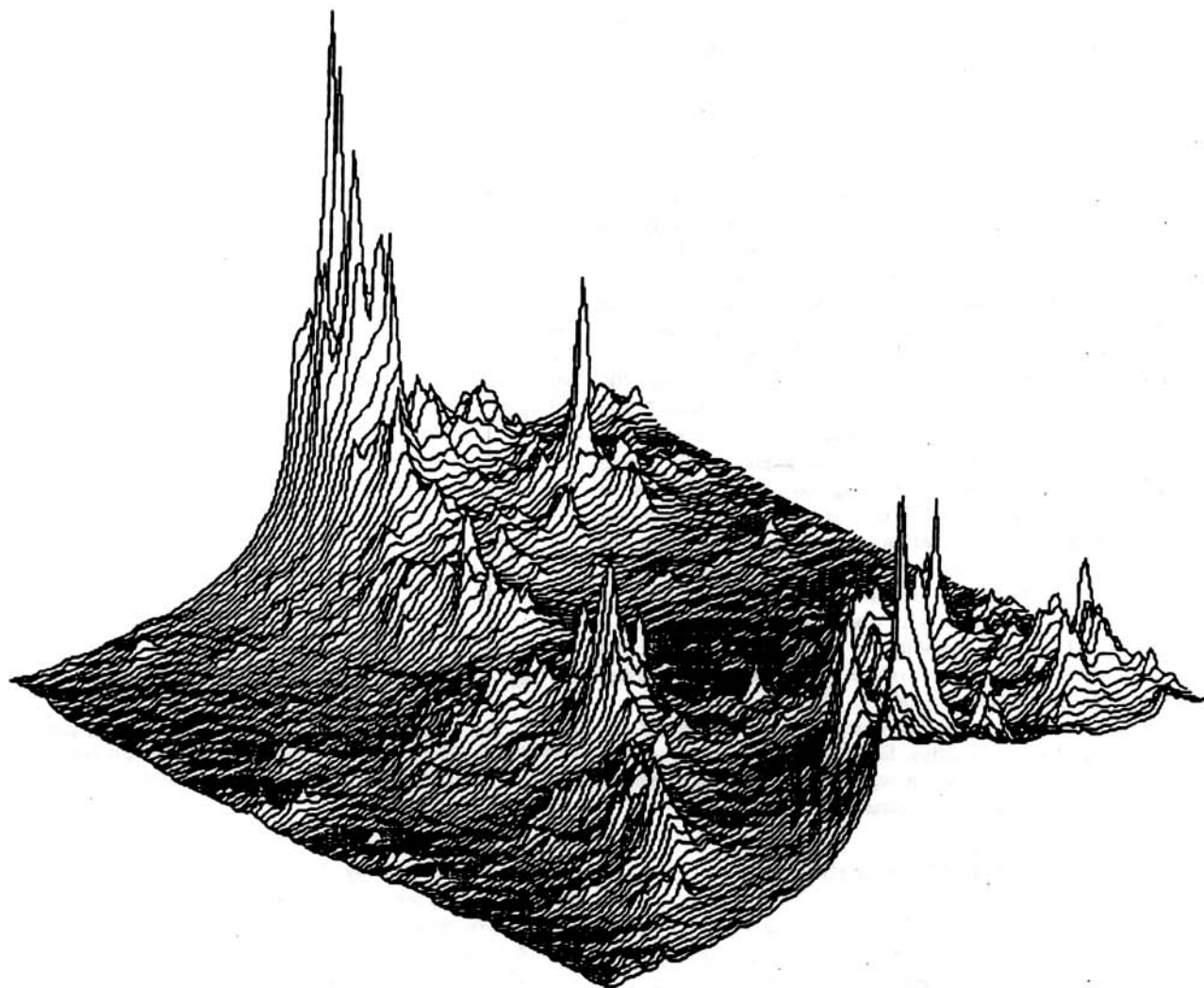
Fig. 6c. The same realization as Figure 6b, but smoothed by fractional integration of order (1/3) to represent the field of a passive scalar "cloud" (see section 2).

size L, and considering $\eta=0$) will approximately hold, as long as $\Lambda=L/\eta \gg 1$ (i.e., we remain near the limiting behavior $\eta \rightarrow 0$). For example, the hth moments for $h \geq \alpha$ will be of the order of $\Lambda^{(h-1)[C(h)-D(A)]}$ (rather than ∞), which diverges as expected as $\Lambda \rightarrow \infty$. Similarly, in order to compare the cascade model with data, we must average the model over a range of scales $\Lambda \gg 1$ where Λ is the averaging length measured in pixels (or in units of model resolution). Hence to give interesting results, the model must be simulated on grids with large ranges in scale.

6. AN EMPIRICAL STUDY OF SCALE INVARIANCE AND MULTIPLE SCALING IN THE RAIN FIELD

6.1. Empirical Studies of Cascades

Atmospheric cascades are fundamentally four-dimensional (space-time) processes involving a hierarchy of fractal sets of dimension generally decreasing to zero (for the most intense singularities). It is clear that the dressed properties depend directly on the dimension of the measuring set ($D(A)$). To obtain the most complete information about the process, we therefore require $D(A)$ to be as large as possible

(since subsets with any smaller dimension can be readily obtained; for another argument for $D(A)=4$, see the discussion of the intersection theorem that follows).

With the possible exception of some experimental Doppler measurements of the wind field, the radar rain reflectivity field is probably the only geophysical data set with $D(A)=4$. For comparison, aircraft have $D(A)=1$, and in situ surface networks have $D(A)<3$ (≈ 2.75 for the World Meteorological Organization measuring network, see Lovejoy et al., [1986a, b] and Montariol and Giraud, [1986]). Most satellite data has no vertical resolution and is thus characterized by $D(A)=2$ or, for those satellites that have temporal resolution high enough to be comparable to their spatial resolution, $D(A)=3$. Hence given the present state of the art in measurement technique, rain measurements have this significant advantage. From a theoretical point of view the chief drawback is that the relationship of the measured reflectivity to the actual cascaded quantity is not very clear.

As argued in the previous sections, all empirical studies of cascade processes must face the fundamental problem that the empirically accessible quantities are "dressed," whereas the

physical processes that generate the cascade determine only the bare quantities directly. In the following we are therefore required to make several approximations in order to estimate the interesting functions $C(h)$, $c(\gamma)$.

6.2. The Data Set

The rain drops scatter microwaves efficiently enough to allow the three-dimensional rain structure to be quickly and nonperturbatively sampled. The data discussed in this paper are taken from the McGill weather radar observatory and consist of "volume scans" (technically called CAZLORs for Constant Altitude Z Log Range maps) of radar reflectivity with a resolution of 0.96° in azimuth and ≈ 1 km in the radial and vertical directions. Each (r, θ, z) scan involves 200 times 375 times 8 ($=600,000$) points, and takes about 3 min to collect (a full radar "volume" scan actually consists of 13 conical scans at increasing elevation angles φ. To obtain (r, θ, z) coordinates, the original (r, θ, φ) data is appropriately resampled). The observatory has archives containing nearly a thousand magnetic tapes representing the last 5 years of continuous operation. The data are digitized on a 4-bit (16-level) log reflectivity Z scale with 4 dBZ ($=$ factor of ≈ 2.5) resolution. The whole scale therefore spans a range of 15 times $4=60$dBZ$=$ factor of 10^6. It is not uncommon for reflectivity levels in rain to exceed 10^5 times the minimum detectable signal.

Physically, the reflectivity is simply the integrated backscatter of the rain drops. Since the microwave scattering cross section (here at 10 cm wavelength) is proportional to the raindrop volume V, the measured

$$Z = \left| \int_A V^2 \exp(i\mathbf{k}.\mathbf{r}) d^{D(A)}x \right|$$

for a drop at position r, wave vector k, and A is the "pulse" volume (here of spatial dimension $D(A)=3$) that is roughly 1 km^3. At 10 cm, the absorption cross section is so low that the beam is nearly unattenuated, yielding accurate estimates of Z. Operational (meteorological) use of radar data is limited primarily by the fact that the rain rate is a very different integral

$$R = \int_A V f(V) d^{D(A)}x$$

where $f(V)$ is the fall speed. The standard semiempirical (and very rough) relationship between R and Z is called the Marshall-Palmer formula: $Z=200R^{1.6}$, with Z in units of (mm)^{5}m^{-3}, and R in millimeters per hour. It is important to note that by directly studying relative reflectivities rather than R, we avoid nearly entirely the radar calibration problem. Noise and instrumental biases are therefore very small.

It is worth pointing out that scaling in Z implies scaling in R, since a characteristic size in one of the quantities would manifest itself in the other. However, if the Marshall-Palmer relation holds and if Z is considered a cascade quantity, then we can go further and conclude that the generators of R and Z are linearly related.

6.3. Divergence of Moments

As shown in section 4, whenever $D(A)<C(h)$, we obtain divergence of hth-order moments and, since $C(h)$ is a
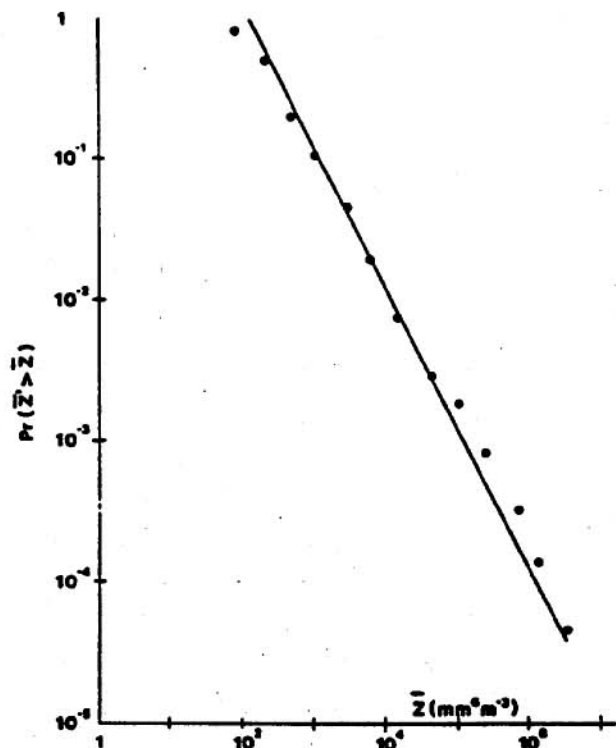

Fig. 7. The probability $Pr(Z'>Z)$ of exceeding a fixed reflectivity threshold Z, sampled from 10 CAZLORs. The straight line has slope 1.06, indicating moments greater than this diverge.

decreasing function, for each $D(A)$ there is a critical value of h, (denoted α), given by $C(\alpha)=D(A)$ such that all moments of order $k\geq\alpha$ diverge. We have already discussed evidence for such a divergence in radar-estimated storm-integrated rainfall, where Lovejoy [1981] obtained $\alpha_R=5/3$. Other estimates of critical exponents in atmospheric fields include $\alpha_v\approx 5$, $\alpha_{tke}\approx 10/3$, $\alpha_\varepsilon\approx 5/3$, $\alpha_{Ri}\approx 1$ [Schertzer and Lovejoy, 1985b], $\alpha_T\approx 5$, [Lovejoy and Schertzer, 1986a; Ladoy et al., 1986], $\alpha_{CO2}\approx 5$ [Visvanathan, 1985] where v indicates velocity, θ potential temperature, ε the energy dissipation, Ri the Richardson number, and CO_2 the concentration of CO_2.

In Figure 7 we show a probability distribution of radar reflectivity density of rain (denoted Z) obtained by pooling data from 10 different 3-km altitude CAZLORs. The line shown has a slope ($=-\alpha$) corresponding to $\alpha=1.06$, indicating that the mean reflectivity density $\langle Z\rangle$ (narrowly) converges (the value 1.06 was determined in a slightly different way from a seperate data base of 70 CAZLORs described in section 6.4). To roughly judge its significance for the rain field, we note that according to the Marshall-Palmer formula, we expect all moments greater than 1.6 times 1.06 ($\approx 5/3$) to diverge, a number that is consistent with the radar-determined storm-integrated value of ≈ 1.65 reported by Lovejoy [1981] which was obtained in Montreal, Spain, and the tropical Atlantic.

6.4. Estimating the Trace Moments

In section 4 the divergence of the usual (dressed) moments was shown to be related to the behavior of the trace moments which were easier to handle. Via the second characteristic functional ($K(h)=(h-1)C(h)$) they are directly
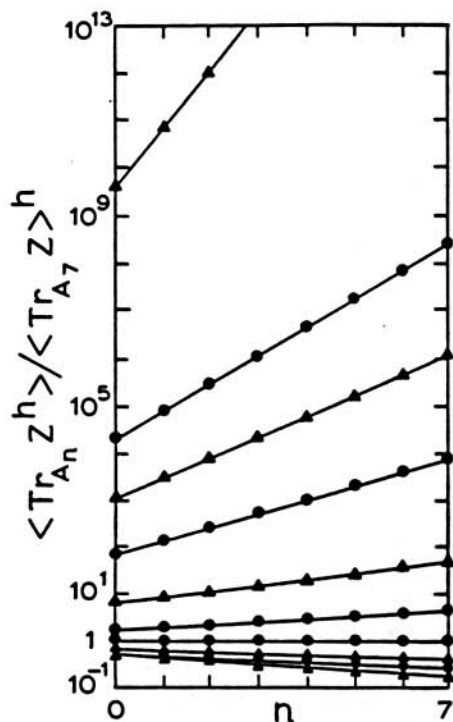
Fig. 8a. The trace h₄ moments estimated from 70 near-independent CAZLORs in the horizontal, with measuring set A a one-dimensional straight line, with log size indicated as ordinate. The straight lines from top to bottom indicate the scaling, their negative slope is the function $p(h)$, for h equal to 5, 3, 2.5, 2,1.5, 1.2, 1, 0.8, 0.6, and 0.3, respectively.

related to the generator of the cascade. To empirically estimate these moments and hence $C(h)$, we follow a series of approximations.

The most important approximation is the estimation of the ensemble averages by sums of independent empirical samples

$$< \cdot > = \left\{ \frac{1}{N} \sum_{j=1}^{N} \cdot \right\} \qquad (37)$$

where N is the number of elements size l_n in the sample (assumed to contain many independent realizations).

Now, we estimate the behavior of the trace moments of Z at resolution l_n (as discussed in Appendix B)

$$Tr_{An} Z_n^h = \int_{An} Z_n^h \, d^{hD(A)} x \propto l_n^{-K(h)+(h-1)D(A)} \qquad (38)$$

Where A_n is the measuring set A at resolution l_n (obtained, for example, by a covering of the set with cubes of size l_n), and Z_n is the "homogenized" Z obtained by spatial averaging over the same cubes. This yields

$$\frac{<Tr_{An} Z_n^h>}{<Tr_{Am} Z_m^h>} \propto l_{n-m}^{-p(h)} \qquad (39)$$

where $p(h)$ is our estimate of the theoretical exponent $K(h)-(h-1)D(A)$ in (38) (except when $h>\alpha$, see following discussion).

The law of large numbers assures us that the effect of replacing ensemble averages by empirical averages over sums is not serious, provided that the former are finite. However, as discussed by *Schertzer and Lovejoy* [1983a, 1984] in the context of wind tunnel data, when $h>\alpha$, the

sums (equation (37)) no longer converge to a number (as $N \to \infty$), but rather to a random (Stable-Levy) variable whose amplitude diverges as $\{l_n^{-D(A)} N\}^{1/\alpha(\alpha-1)}$ as $N \to \infty$. For fixed N, we also obtain the following spurious scaling exponent

$$p(h) \approx \frac{D(A)(h-\alpha)}{\alpha} \qquad h \ge \alpha \qquad (40)$$

In this case the experimental codimension $C_e(h)=p(h)/(h-1)$ is no longer a good estimate of the true codimension $C(h)$. In particular, we obtain a spurious value

$$C_{e\infty} = \frac{D(A)}{\alpha} \qquad (41)$$

This spurious scaling (see *Lavallée et al.* [1987] for a more detailed discussion) is important for two reasons. On the one hand, it masks the actual divergence of moments (which cannot be directly observed, since the empirical values of necessity have finite N) and therefore underestimates the $C(h)$ (which need not even be bounded). On the other hand, it gives us another, more precise method of determining $\alpha(A)$ (the critical exponent for the set A, dimension $D(A)$), by studying the asymptotic behavior of $p(h)$, for $h >> \alpha(A)>1$), by using (41).

Figure 8a and 8b show the (normalized) trace moments $(TrZ_n^h/(TrZ_8)^h)$ estimated in this way for 70 horizontal radar images ($D(A)=1$, 2 respectively) with $n=1$, 8; hence for a range of scales, $\lambda^{n-1}=2^7=128$. Using the normalized ratio is equivalent to normalizing the field so that $<Z>=1$. The straightness of the lines shows that scaling is accurately followed. Perhaps the most striking point to notice is the significant difference between $D(A)=1$ and $D(A)=2$ (Figure 8a and 8b respectively). This is an immediate consequence of the multiple scaling and is readily understood with the aid of a simple intersection theorem, shown in Figure 9. If we
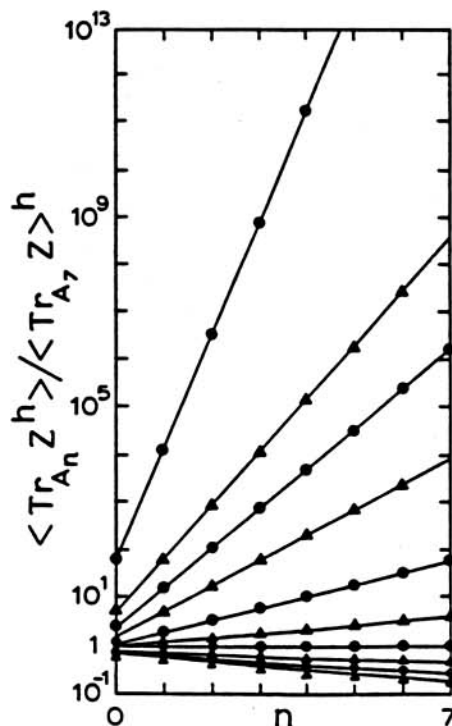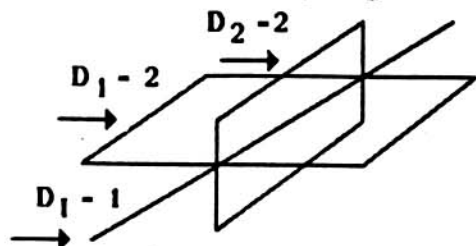

Fig. 8b. Same as Figure 8a, but for A in the two-dimensional (horizontal) plane.

THE INTERSECTION THEOREM:

Two sets, dim -D_1, D_2 embedded in a space

dim - E, intersect on a set dim - D_I.

Define the *Co-dimension* C-E- D.

> **THEOREM:**
> $$C_I - Inf ((C_1 + C_2), E)$$

Ex. Intersection in space (E-3) of two planes
(D_1- D_2- 2 $\Rightarrow$ C_1- C_2-1)

$$C_I - C_1 + C_2 - 2 \Rightarrow D_I - E - C_I - 1$$

Fig. 9. A schematic diagram showing the intersection theorem for two sets (here planes). The general rule is that the codimension of an intersection is the sum of the codimensions, of the intersectting sets.

consider the rain field to consist of a hierarchy of nested fractals, with dimension increasing with intensity, then averaging over a set A with $D(A)<d$ (the dimension of the space in which the process occurs), will miss (fail to intersect) all fractals with $D<d-D(A)$ (=$C(A)$). As we decrease $D(A)$, more and more of the low-dimensional fractals are missed, hence altering the statistical properties of the averages.

We now turn to the interpretation of Figure 8b, which we take as an estimate of the two-dimensional trace moments. Figure 10a shows the function $p(h)$ obtained as its negative slope. For $h<1$, $p(h)$ is negative, in conformity with the sign of $(h-1)$. For $h>1$, $p(h)$ quickly asymptotes to a straight line (as expected since $\alpha_z \approx 1.06$). The theoretical lines corresponding to $\alpha=1.05$ and $\alpha=1.075$ are shown for reference; the actual curve passes through them. These provide fairly accurate bounds on α_z; we estimate $\alpha_z=1.06\pm0.02$. Using the formula $C(h)=p(h)/(h-1)$, we obtain Figure 10b. Recall that for $h\geq\alpha$ the values are not true codimensions.
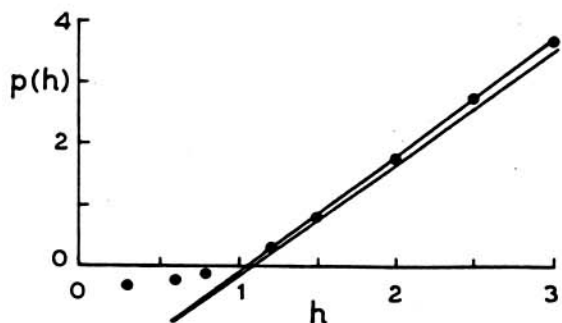
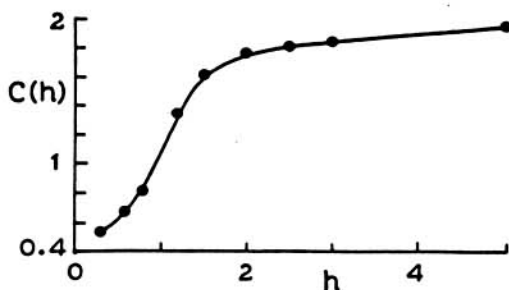Fig. 10a. The function $p(h)$ for the data corresponding to Figure 8b.

Fig. 10b. The codimension function $C(h)$ corresponding to the data used in fig. 8b, obtained as $C(h)=p(h)/(h-1)$.

6.5. Empirical Estimates of the Dimensions of the Singularities

We have argued that the codimensions of the sets over which the singularities of various orders are distributed ($c(\gamma)$) are related to the moment codimension function ($C(h)$) by a Legendre transformation. Although such a method of obtaining $c(\gamma)$ from $C(h)$ has been used in studies of strange attractors [e.g., *Halsey et al.* 1986], it is of little use here, since over most of the range of h, the empirical function $C_e(h)$ is a poor estimate of the true $C(h)$ because of the divergence of moments for $h>1.06$. It is therefore of interest to develop a complimentary method that can be directly applied to individual realizations, rather than to ensemble averages.

Rather than estimating bare moments at scale l_n by "homogenizing" the dressed moments via appropriate spatial averaging, here we fix the resolution of the data at the smallest accessible scale (l_n) and associate each intensity level (or threshold) T in the data with singularities of order γ, as follows

$$T=l_n^{-\gamma} \qquad (42)$$

In this way each intensity level corresponds to a singularity of a well-defined order; determining the function $D(T)$ (the dimension of regions exceeding T) allows us to determine $c(\gamma)=d-D(T)$, (where as usual, d is the dimension of the space).

The simplest way of evaluating $D(T)$ is to generalize the standard procedure for estimating dimensions of strange sets, called "box counting." Box counting is based on the notion of covering used in defining the Hausdorff measure of a set (it is not exactly the same, however, the resulting dimension is only an estimate of the Hausdorff dimension). If $N(L)$ is the number of disjoint cubes (of approriate dimension) of size L needed to cover the set, then the dimension D is given by $N(L)\approx L^{-D}$. Applying this algorithm to the thresholded field, we obtain a functional version of the box-counting algorithm (called "functional box counting" by *Lovejoy et al.*, [1987] see Figure 11).

Lovejoy et al., [1987] give a detailed discussion of this technique when applied to 20 radar CAZLORs (see also *Lovejoy and Schertzer*, [1986a], and *Gabriel et al.*, [1986] for applications to satellite cloud pictures). The method clearly confirms that over the entire radar accessible range of several kilometers to several hundred kilometers, that scaling is very accurately followed on individual CAZLORs for reflectivities varying by a factor of $\approx$40,000. The functional box-counting method is statistically quite robust because it converts the wildly varying reflectivity field into a binary

FUNCTIONAL BOX COUNTING

The dimension D(T) of regions
exceeding threshold T:

$$N_T(L) \subset L^{-D(T)}$$

$N_T(L)$ is the number of boxes size L needed
for the cover

original field with →
isolines $T_2 > T_1$

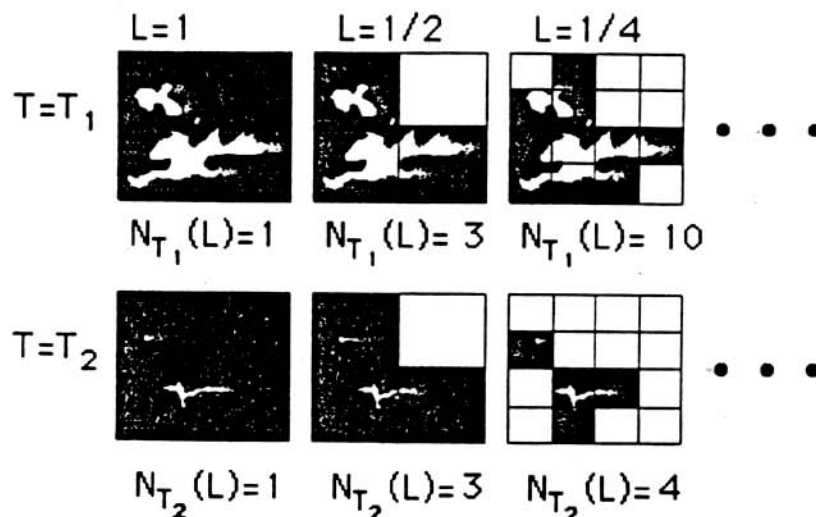|	L=1	L=1/2	L=1/4	
T=T$_1$				•••
	$N_{T_1}(L)=1$	$N_{T_1}(L)=3$	$N_{T_1}(L)=10$	
T=T$_2$				•••
	$N_{T_2}(L)=1$	$N_{T_2}(L)=3$	$N_{T_2}(L)=4$	

Fig. 11. A schematic diagram illustrating functional box-counting.

(above/below threshold) field (which is then viewed as a set). However, as it still relies on the dressed quantities, we run into exactly the same problem as for the trace moments: for T sufficiently large (high enough order singularities), the bare quantities (and hence dimensions) are no longer even approximated by the dressed ones, hence we still don't obtain full information on the generator ($C(h)$) of the cascade. *Gabriel et al.* [1987] use this method to estimate $c(\gamma)$ for radar data as well as satellite infrared and visible radiances from 8 to 512 km, and show that the functions $c(\gamma)$ fall into the universality classes discussed in C2.

By extending functional box counting to anisotropic boxes (a method called "elliptical dimensional sampling"), *Lovejoy et al.*, [1987] were able to estimate directly the elliptical dimension characterizing the vertical stratification in rain, obtaining the value $d_{el}=2.22\pm0.07$.

7. CONCLUSIONS AND SUMMARY

Motivated by the undeniable necessity of achieving a better turbulent treatment of rain and cloud fields, we argued that the relevant nonlinear dynamical processes can best be simulated stochastically. Starting with the study of a passively advected cloud, we showed how a (multiplicative) cascade treatment offers a new and concrete way of

theoretically investigating as well as modeling these fields. This approach enabled us to show that each of the fluctuating fields may be generated by a fractional integration of products of interacting conserved fluxes (in particular, of energy and water substance) raised to various powers.

For each flux we outlined the central features, both of the bare cascade properties obtained after only a finite number of cascade steps, and of the dressed properties obtained by averaging a completed cascade process. This fundamental distinction arises from the very singular small-scale limit of multiplicative cascade processes. In real cascades, viscosity eventually damps out fluctuations; however, whenever averages are taken over scales much larger than the viscous scale, the limiting behavior is nearly obtained. In the atmosphere, averages over meters already involve scale ratios of the order of a thousand and are dominated by the singular limit. Hence, for example, if we consider the hth power of fluxes over a set A, with $h \geq \alpha(A)$, and where the singular limit leads to divergence, in a real cascade, very large values will be obtained that depend critically on the very small-scale details. This is completely different from the usual situation (which still holds for $h < \alpha(A)$) where the statistical properties are governed by the large scale. This is important when measuring fluxes since empirical estimates of powers of fluxes with $h < \alpha(A)$ will converge to

well-defined limits (if the sampling is adequate), whereas they will always be dominated by "outliers," and hence remain ill defined, when $h > \alpha(A)$.

These basic structural properties of the cascades are preserved for interacting fluxes, hence they are essential for both cloud and rain modeling and analysis. In particular, it was noted that the interactions between the different fields were very simply expressed in terms of the generators of the different cascades. In anticipation of future developments, we explicitly showed how to construct cascade models of clouds and rain. By generalizing these methods to vector fields, we may expect to be able to simulate the velocity field itself.

An important part of this paper (see section 6), was concerned with the empirical testing of the theory, particularly as concerns the divergence of moments, multiple scaling, and multiple dimensions. The data chosen for our study were radar rain reflectivities which have very low noise over a wide range of space and time scales. We first analyzed the divergence of moments of the reflectivities by empirically determining the probability distribution of volume-averaged reflectivities, obtaining $Pr(Z' > Z) \sim Z^{-\alpha}$, with $\alpha \sim 1.06$ for the probability of an extreme reflectivity Z' exceeding a fixed value Z (note that all moments higher than the value 1.06 therefore diverge).

To investigate the multiple scaling and multiple dimensions predicted by our theory, we developed new data analysis techniques involving trace moments and functional box counting. The former gives direct information about how the various moments of the field depend on both the scale and dimension over which they are averaged. The latter determines the fractal dimensions associated with various intensity levels (defined by thresholds), which in turn correspond to the various orders of singularities in the field. It is also used as the basis of yet another technique (summarized in Appendix D), called "elliptical dimensional sampling," to estimate the elliptical dimension of the rain field. The value obtained ($= 2.22 \pm 0.07$) is between the value 3 (corresponding to an isotropic rainfield), and 2 (corresponding to a completely stratified two-dimensional field).

Overall, various new tools for the study of intermittent fields have been presented, discussed, and tested. They may be expected to have many immediate practical implications, especially for the prediction, detection and measurement, and modelling of turbulent fields. The present study points to new theoretical approaches that directly exploit the extreme intermittency.

APPENDIX A: SCALING SYMMETRIES OF THE DYNAMICAL EQUATIONS OF PASSIVE ADVECTION

We start from the incompressible Navier-Stokes equations, which prescribe momentum conservation, and the equation of (passive) advection

$$\partial v / \partial t = [1 - P(\nabla)] v \nabla v - v \Delta v + f$$
$$\nabla v = 0 \tag{A1}$$
$$\partial \rho / \partial t = f' - v \nabla \rho - \kappa \nabla^2 \rho$$

where v is the velocity, ρ the passive scalar concentration, t the time, f and f', the (solenoidal) external forcings (partially representing the boundary conditions), v the kinematic viscosity, κ the scalar diffusivity, and $P(\nabla)$ is the

curl-free projection, namely:

$$P_{i,j}(\nabla) = \nabla^{-2} \nabla_i \nabla_j \tag{A2}$$

Equation (A1) has the nice formal property of being scaling (or scale invariant), i.e., invariant under scale transformation of the form

$$
\begin{array}{lll}
x \rightarrow \lambda x & t \rightarrow \lambda^{1-H} t & P \rightarrow P \\
v \rightarrow \lambda^H v & v \rightarrow \lambda^{H+1} v & f \rightarrow \lambda^{2H-1} f \\
\rho \rightarrow \lambda^H \rho & \kappa \rightarrow \lambda^{H+1} \kappa & f' \rightarrow \lambda^{H+H'-1} f'
\end{array}
\tag{A3}
$$

The basic problem is to give a precise meaning to this formal transformation. It is usually expressed in statistical terms, e.g., the "characteristic" fluctuations $\Delta v(l)$, $\Delta \rho(l)$ at scale l are amplified by the factors λ^H and $\lambda^{H'}$ respectively when the length scales are stretched by the factor λ. H and H' are determined as soon as we assume statistical isotropy and homogeneous transfer rates (per unit of volume and mass) of energy and scalar variance, both of which are conserved by nonlinear interractions

$$
\begin{aligned}
\varepsilon &= \partial(\Delta v(l))^2 / \partial t = \text{constant} \\
\chi &= \partial(\Delta \rho(l))^2 / \partial t = \text{constant}
\end{aligned}
\tag{A4}
$$

where $H = H' = 1/3$. This corresponds to a power law energy spectrum

$$E(k) \sim k^{-\beta}$$
$$\beta = 2H + 1 \tag{A5}$$

since

$$\Delta v(l) \sim k \ E(k); \quad k \sim l^{-1} \tag{A6}$$

APPENDIX B: TRACE MOMENTS AS HAUSDORFF MEASURES

On any compact set A the D-dimensional Hausdorff measure is defined as follows:

$$\int_A d^D x = \lim_{\delta \to 0} \inf_{\substack{UB_i \supset A \\ \left(\int_{B_i} d^D x\right)^{1/d} \leq \delta}} \sum_i \left(\int_{B_i} d^d x\right)^{D/d} \tag{B1}$$

(i.e., the infimum is over all coverings with balls B_i with a diameter less than or equal to δ). With cubic discretization (used in section 3.2), we have:

$$\int_A d^D x = l_0^D \lim_{\substack{m \to \infty}} \inf_{\substack{UB_{m,J} \supset A \\ \min}} \sum_{B_{m,J}} \left[\lambda^{-mD} \right] \tag{B2}$$

(where the balls $B_{m,J}$ are taken here to be cubes, size $l_0 \lambda^{-m}$ centered at x_J).

One may note that the "box-counting algorithm" (used in section 3 and discussed in section 6), which assumes that the minimum number of cubes required to cover a fractal set can be obtained by cubes of the same size l ($= \lambda^{-m}$) behaves as

$$N(l) \sim l^{-D} \tag{B3}$$

which approximates (B2) (to within a logarithmic correction, see *Mauldin and Williams* [1986]).

For integer h and temporarily considering ε as an ordinary function, the hth power of the flux can be written as

$$\Pi^h = \int_{x_1 \in A} \cdots \int_{x_h \in A} \varepsilon(x_1) \cdots \varepsilon(x_h) d^{D(A)} x_1 \cdots d^{D(A)} x_h \quad \text{(B4)}$$

where the integrand is an hth-order tensor and equation (34) can be rewritten as follows:

$$Tr_A \Pi^h = \int \cdots \int \varepsilon(x_1) \cdots \varepsilon(x_h) d^{D(A)} x_1 \cdots d^{D(A)} x_h \quad \text{(B5)}$$
$$x_1 = \cdots = x_h \in A$$

$Tr_A \Pi^h$ is therefore the tracelike component of the hth power of the flux (obtained by summing over $\varepsilon^h(x)$, the diagonal of $\varepsilon(x_1) \varepsilon(x_2) \ldots \varepsilon(x_h)$). Now, we give a precise meaning to the right hand side of the latter equation when ε is no longer a function but results from a cascade process

$$Tr_A \Pi^h = \lim_{n \to \infty} \inf_{\substack{UB_{m,J} \supset A \\ m \geq n}} \sum_{B_{m,J}} \left[\Pi_m^h(B_{m,J}) \right] \quad \text{(B6)}$$

i.e., the elementary volume ($d^{D(A)} x$) involved in the definition of Hausdorff measure equation (B2) is replaced by $\{\varepsilon(x) d^{D(A)} x\}^h$. This allows us to keep the previous notation for the trace of Π^h, even when ε is no longer a function but an operator. One may already note that due to the above properties of Hausdorff measures, the trace of homogeneous flux will vanish for $h>1$. The singularities of inhomogeneous fluxes leads to a very different behavior.

Considering now the trace moments, the multiple scaling of ε_n ($\langle \varepsilon^h \rangle \sim l^{-K(h)}$, where $K(h) = (h-1)C(h)$ is the second characteristic function of the generator of the cascade and is convex; $C(h)$ is an increasing function which merely changes the dimension of the integrand, since

$$\langle \Pi_m^h(C_m) \rangle \sim L_m^{D(A)-(h-1)[C(h)-D(A)]} \quad \text{(B7)}$$

this scaling leads to:

$$\langle Tr_A \Pi^h \rangle = \int_A d^{D(A)-(h-1)[C(h)-D(A)]} x \quad \text{(B8)}$$

provided that no difficulty arises from taking the limit ($n \to \infty$, $m \geq n$) in equation (B6) (anticipating the following, this means avoiding the degenerate case). With this proviso the simple divergence rule of the Hausdorff measure leads to a twin-divergence rule for the trace moments, ruled by the two zeros of the convex function $(h-1)[C(h)-D(A)]$.

We may then exploit the fact that $\left(\sum_i x_i^h \right)^{1/h}$ is a decreasing function of h in order to obtain the basic inequalities relating trace and usual moments of the flux:

$$\langle Tr_A \Pi^h \rangle \leq \langle \Pi(A)^h \rangle \leq \langle Tr_A \Pi^h \rangle + R_A(h) \quad h \geq 1 \quad \text{(B9)}$$

$$\langle Tr_A \Pi^h \rangle \geq \langle \Pi(A)^h \rangle \quad h \leq 1 \quad \text{(B10)}$$

where $R_A(h)$ is the remainder that involves finite sums over lower order moments of the flux.

As discussed by *Schertzer and Lovejoy* [1987], inequality (B9) implies that high-h ($h>1$) divergence of the trace moments is equivalent to the divergence of the tensor moments. In contrast, inequality (B10) is important when considering possible degeneracy of the process, i.e., when ε_n is almost surely everywhere null (for n large enough, the singular behavior of ε_n occurs on a vanishingly small set). In particular, a low-h divergence ($h<1$) is required to avoid degeneracy and to assure the self-consistency of the preceeding derivation.

In practical applications it is important to note that the trace moments can be crudely approximated by various expressions involving the set A at resolution l_n (denoted A_n with $A_n = U B_{n,J}$ where $B_{n,J}$ are disjoint covering balls). This means replacing A by a (minimum) covering of cubes of size l_n. The trace moments can then be obtained from either the bare flux Π_n or from the dressed flux π homogenised over the same scale:

$$Tr_{A_n} \Pi_n^h = \sum_{B_{n,j}} \Pi_n(B_{n,j})^h$$
$$\quad \text{(B11)}$$
$$Tr_{A_n} \Pi^h = \sum_{B_{n,j}} \Pi_n(B_{n,j})^h$$

The trace moments are then obtained by ensemble averaging. We may expect that the two will differ only by a logarithmic divergence, as long as $h < \alpha(A)$, and that in this regime the scaling behavior of the two will be the same.

APPENDIX C: CONTINUOUS MULTIPLICATIVE PROCESSES.

C.1. *The 1/f Noises as Generators of Multiplicative Processes*

Continuous cascade processes correspond to the (bare) energy-flux density ε_λ down to scale l/λ defined for any $\lambda > 1$, still satisfying the (now continuous) scaling property

$$\varepsilon_{\lambda\lambda'} = \{T_{\lambda'}(\varepsilon_\lambda)\} \varepsilon_{\lambda'} \quad \text{(C1)}$$

with $T_{\lambda'}$ being the contraction of ratio $1/\lambda'$. Turning to the infinitesimal generator of the (semi) group ε_λ, we are led to the same (group) properties as for the discrete group for finite exponential increments

$$\Gamma_{\lambda\lambda'} = T_{\lambda'}(\Gamma_\lambda) + \Gamma_{\lambda'}$$
$$\varepsilon_\lambda = \frac{e^{\Gamma_\lambda}}{\langle e^{\Gamma_\lambda} \rangle} \quad \text{(C2)}$$

Γ_λ and ε_λ will be noises of maximal wave number λ/l_o (this is a new explicit definition of the scale of homogeneity) which is easier to study in Fourier space. In the following, Fourier transforms of physical space quantities (e.g., $\Gamma_\lambda(x)$) will be denoted by a circonflex (e.g., $\hat{\Gamma}_\lambda(k)$), k indicating a wave vector and k ($=|k|$) the corresponding wave vector, and we will take, for sake of notational simplicity, $l_o=1$. We have the following relationship between infinitesimal ($\hat{\gamma}$) and finite ($\hat{\Gamma}_\lambda$) exponential increments:

$$\hat{\Gamma}_\lambda(k) = \hat{\gamma}(k) \hat{1}_{s\lambda}(k) \quad \text{(C3)}$$

$\hat{1}_{s\lambda}$ being the indicator function of the spherical (hyper) volume S_λ delimited by the spheres of radius 1 and λ, both centered at the origin of Fourier space ($\hat{1}_{s\lambda}(k) = 1$ if $1 \leq k \leq \lambda$, 0, otherwise). In the subsection C.2 we show that the infinitesimal generator of a scaling multiplicative process must be a "1/f noise" (i.e., frequency spectrum proportional to the inverse of the frequency; here frequency has to be replaced by wave number) with either Gaussian or Levy-stable statistics.

In order to have multiple scaling the characteristic functionals K and $\hat{K}$ of Γ_λ and $\hat{\Gamma}_\lambda$, respectively, must be logarithmically divergent, namely:

$$K_{\Gamma_\lambda}(h\delta) = \hat{K}_{\hat{\Gamma}_\lambda}(h\hat{1}) = \log \lambda K(h) \quad \text{(C4)}$$

due to the fact that the unit function ($\hat{1}$) is the Fourier transform of the Dirac function δ. Let us check that in a very general manner the spectrum $E\hat{1}_\lambda$ of $\hat{1}_\lambda$ is defined by

$$\hat{K}_{\hat{1}_\lambda}(\hat{1}) = \int_1^\lambda E\hat{1}_\lambda(k)\, dk \qquad (C5)$$

Indeed, let $\hat{\Gamma}_{\alpha\lambda}$ be defined as

$$\hat{\Gamma}_{\alpha\lambda}(k) = \hat{f}(k)\, \hat{\gamma}_\alpha(k)\, \hat{1}_\Omega(k) \qquad (C6)$$

$\hat{\gamma}_\alpha(k)$ being a (unitary) white noise, either Gaussian ($\alpha=2$) or Levy-stable of index α ($1<\alpha<2$). Namely, we consider the $\hat{\gamma}_\alpha(k)$ for the different k, to be independently identically distributed according to a symmetric law, either Gaussian ($\alpha=2$) or Levy-stable (of index α), with a "unitary" characteristic function in the sense that for any complex u equals

$$\hat{K}_{\hat{\gamma}_\alpha(k)}(u) = \log[<\exp(u\hat{\gamma}_\alpha(k))>] = |u|^\alpha \qquad (C7)$$

[Feller, 1971]. Note that we have used the traditional Levy-stable parameter α; it should not be confused with the quite different α used in the α-model. As (C7) implies,

$$\hat{K}_{\hat{\gamma}_\alpha}(\hat{f}) = K^{(\alpha)}(\hat{f}) = |\hat{f}|_\alpha{}^\alpha$$

$$|\hat{f}|_\alpha = \left\{ \int |\hat{f}(k)|^\alpha\, d^d k \right\}^{1/\alpha} \qquad (C8)$$

when $\hat{f}$ has a finite α-norm ($|\hat{f}|_\alpha < \infty$), more generally,

$$\hat{K}_{\hat{\Gamma}_\alpha}(\hat{f}) = \left| \hat{1}_\Omega \hat{f} \right|_\alpha{}^\alpha \qquad (C9)$$

hence

$$E\hat{1}_\lambda(k) = \int_{\partial S_\lambda} |\hat{f}(k)|^\alpha\, d^{d+1}k \qquad (C10)$$

∂S_λ being the outer frontier of S_λ (i.e., the (hyper) surface of the sphere of radius λ), corresponding to the usual definition of the spectrum in the Gaussian case and to its natural extension for Levy-stable noises. According to (C5) and (C10), the required logarithmic divergence of K and $\hat{K}$ corresponds to γ being a "$1/f$ noise", i.e.

$$E_{\hat{\gamma}(k)}^\wedge = \frac{k^{-1}C_1}{(\alpha-1)}$$

$$\hat{\gamma}(k) = \left[\frac{k^{-d}C_1}{(\alpha-1)} \right]^{1/\alpha} \hat{\gamma}_\alpha(k) \qquad (C11)$$

$\hat{\gamma}_\alpha(k)$ still being a (unitary) white noise, either Gaussian ($\alpha=2$) or Levy-stable ($1<\alpha<2$)).

C.2. Universal Properties and Codimension Functions

In order to clarify the discussion we will call the (previously defined) white noises "subgenerators", since specific generators of cascade processes $\hat{\gamma}(k)$ are obtained by fractional integrations over them (multiplying them by a noninteger power of the wave number (equation (C10)). These subgenerators have the same properties of stability and attractivity, under addition, as the Gaussian and Levy-stable variables (see for example Feller [1971]), as could be easily inferred from the similarity between the characteristic function and functional (Equations (C7) and

(C8)). Namely, the sum ($i=1, \infty$) of i.d.d. (identically independent distributed) white noises $\hat{\gamma}^{(i)}$ (i.e., for each i, the $\hat{\gamma}^{(i)}(k)$ i.d.d. for the different k) will converge toward one of these subgenerators. In that sense the $\hat{\gamma}_\alpha$ represent "universality classes." The critical exponent α of the class toward which the sum of the $\hat{\gamma}^{(i)}$ converges, corresponds to the moment of divergence of the $\hat{\gamma}^{(i)}$

$$\alpha = \inf(\alpha_1,2); \quad 1<\alpha_1\leq\infty; \quad h\geq\alpha_1 < |\hat{\gamma}^{(i)}(k)|^h> = \infty \qquad (C12)$$

Thus the sum of a large number of hyperbolic white noises (with a given α_1) will converge towards a Levy-stable (or Gaussian) white noise. Corresponding "universal" properties hold for the generators themselves (via fractional integration).

The codimension function with a subgenerator $\hat{\gamma}^{(i)}(k)$ is derived from (C4), (C5), (C9), and (C11):

$$C^{(\alpha)}(h) = \frac{K^{(\alpha)}(h) - hK^{(\alpha)}(1)}{(h-1)}$$

$$= \frac{C_1 [h^\alpha - h]}{(h-1)(\alpha-1)} \quad C^{(\alpha)}(1) = C_1 \qquad (C13)$$

for the corresponding critical codimension function of the divergence of moments of the cascade process. In particular, for the Gaussian case

$$C^{(2)}(h) = C_1 h \qquad (C14)$$

Using the fact that h^α/α and $\gamma^{\alpha'}/\alpha'$ (with $1/\alpha+1/\alpha' =1$) are dual Legendre transforms, and that

$$c'(\gamma') = c(\gamma)$$

$$K'(h') = K(h) + \frac{bh}{a}$$

with

$$\gamma' = a\gamma + b$$

$$h = ah'$$

We find that the codimension function of the singularities (of the normalised generator) is given by

$$c^{(\alpha)}(\gamma) = C_1 \left(\frac{\gamma}{\alpha'C_1} + \frac{1}{\alpha} \right)^{\alpha'} \qquad (C15)$$

More generally, the codimension function of the singularities of the field obtained by fractional integration over arbitrary powers of such a generator (e.g., liquid water content) will be of the same type since this corresponds to the above linear transformation of γ. Hence, we may expect $c(\gamma)$ to have the general (universal) form

$$c(\gamma) = c(0) \left(1 + \frac{\gamma}{\gamma_0} \right)^{\alpha'} \qquad (C16)$$

where $c(0)$, γ_0, α' are parameters that can be determined empirically (see Gabriel et al. [1987]).

APPENDIX D: ANISOTROPIC SCALE INVARIANCE

D.1. Outlines of Generalized Scale Invariance

In Appendix A we dealt with isotropic spatial scale transformations (i.e., pure dilations of coordinates). This

was reasonable since as long as the boundary conditions are isotropic the Navier-Stokes and advection equations have no preferred directions. However, in cloud fields or radar rain fields, anisotropy is immediately perceptible as "texture," cloud "type," etc. [*Lovejoy and Schertzer*, 1986b], and the assumption of isotropy is clearly inappropriate. In geophysical flows such as those involved in the rain process, the relevant governing equations (when they are known) involve oriented forces such as buoyancy (due to gravity) as well as the Coriolis force (due to the earth's rotation). These forces, which may introduce anisotropic differential operators, e.g., a fractional differential operator with the order of differentiation depending on the direction instead of (isotropic) gradients, are responsible for the (fractional) differential stratification and rotation of the atmosphere respectively. Figures 2c et 2d point to a way of defining anisotropic scaling via a linear transformation of one rectangle into another, with a scale ratio λ

$$T_\lambda = \lambda^{-G} = \exp(-G \log \lambda) \qquad (D1)$$

G itself being a linear transformation. Unless G is the identity, T_λ is no longer a mere contraction, and rectangles are only self-affine, not self-similar. The consequence of this kind of transformation is that the singularities are no longer evenly distributed on subsets with equal topological and (isotropic) Hausdorff dimensions. For example, as soon as we anisotropically distribute the activity of turbulence (such as in Figures 2c et 2d), a vertical line is no longer equivalent to an horizontal one, etc.

It clearly would be painful and extreme to attempt to continue to use isotropic notions (such as isotropic Hausdorff measures and dimensions) in this type of anisotropic situation. Indeed, the persistant use of isotropic concepts has led (e.g., *Mandelbrot*, [1986]) to the artificial introduction of two quite different scale-dependent isotropic dimensions when a single anisotropic dimension is sufficient for a complete description of a set.

In the following, we give a brief outline of the general anisotropic framework called "generalized scale invariance" (GSI) [*Schertzer and Lovejoy*, 1985a, 1986, 1987; *Lovejoy and Schertzer*, 1985a, 1986a] in order to define Hausdorff measures and the associated dimensions (that we call "elliptical dimensions") in the same anisotropic framework as the process itself, based on a (generalized) notion of scale related to the measurability properties of the process (metric properties are not required at all).

In isotropy, scaling is based on three essential ingredients: (1) a unit sphere; (2) the identity 1 as the generator of the self-similar scale-changing transformation ratio λ, ($T_\lambda = \lambda^{-1}$); and (3) the corresponding scale notion ϕ (the radius of the sphere $S_\lambda = \lambda^{-1} S_1$): $\phi(S_\lambda) = \lambda^{-1} \phi(S_1) = \lambda^{-1}$. Anisotropic scaling is based on the same ingredients, but with $T_\lambda = \lambda^{-G}$ with $G \neq 1$, and $\phi_{el}(T_\lambda S_1) = \lambda^{-1} \phi_{el}(S_1)$. The subscript el is used in the following to refer to the fact that in anisotropy the scale-defining spheres are typically flattened ellipsoids. In fact, much more general shapes are possible; in the nonlinear case they need not even be convex.

The method of getting from the isotropic triple $(S_1, 1, \phi)$ with

$$\phi = \left(\int_A d^d x \right)^{1/d}$$

to the anisotropic (S_1, G, ϕ_{el}) is to test whether the generator

G has the required properties for the self-affine ellipsoids $E_\lambda = T_\lambda(S_1)$ rather than the self-similar spheres. In particular, do the E_λ increase as λ is decreased, and how can one define ϕ_{el}? The answers to both these questions turn out to be simple, on the condition that every (generalized) eigenvalue of G has a nonnegative real part, i.e.,

$$\inf Re\ \sigma(G) \geq 0 \qquad (D2)$$

where $\sigma(G)$ is the (generalized) spectrum of G:

$$\sigma(G) = \{\mu_j \in C \mid G - \mu_j 1 \text{ noninvertible on } C \times R^d\} \qquad (D3)$$

a (nongeneralized) eigenvalue μ_j corresponds to $G - \mu_j 1 = 0$ on its eigen space F_{μ_j} and ϕ_{el} is simply defined as

$$\phi_{el}^{d_{el}}(E_\lambda) = \phi^d(E_\lambda) = \lambda^{d_{el}} \phi^d(S_1) = \lambda^{d_{el}} \phi_{el}^{d_{el}}(S_1) \qquad (D4)$$

with $d_{el} = Tr(G)$. Anisotropic Hausdorff measures of dimension D_{el} are simply defined as

$$\int_A d^{D_{el}} x = \lim_{\delta \to 0}\ \inf_{\substack{A \supset \cup E_i \\ \phi_{el}(E_i) < \delta}} \sum_{E_i} \phi_{el}^{D_{el}}(E_i) \qquad (D5)$$

From equation (D4) $\phi_{el}^{D_{el}}(T_\lambda S_1) = \phi^D(T_\lambda S_1)$, with $D = (d/d_{el})D_{el}$, hence

$$\int_A d^{D_{el}} x_{el} \qquad (D6)$$

is similar to

$$\int_A d^D x \qquad (D7)$$

notwithstanding the difference that the former case involves a covering by ellipsoids (E_i) rather than spheres (S_i) in the latter. Nevertheless, if A is not "strange" (pathological), we may suppose that a near optimum covering (i.e., nearly equal to the infimum above) of ellipsoids can be associated with a near-optimum covering of spheres if each of the ellipsoids is itself covered nearly optimally by smaller spheres. We can therefore expect the divergence rule for D6 and D7 to be the same. We have thus the following rule :

$$D_{el}(A)/d_{el} = D(A)/d \qquad (D8)$$

However, if A is restricted to a (generalized) eigenspace F_{μ_j} of G, then the preceding rule must be rewritten:

$$D_{el}(A)/d_{el\,j} = D(A)/d_j \qquad (D9)$$

where d_j is the topological dimension of F_{μ_j} and $d_{el\,j}$ its anisotropic dimension, i.e., $d_{el\,j} = Tr(G_j)$, with G_j being the restriction of G on F_{μ_j}. More generally, the following relationship will hold for A restricted on a (direct) sum F of F_{μ_j}

$$D_{el}(A)/d_{el}(F) = D(A)/d(F) \qquad (D10)$$

with $d_{el}(F)$ and $d(F)$ being the elliptical and topological dimensions of the subspace F, respectively. This corresponds to the fact, already noted, that subspaces with identical (topological, isotropic Hausdorff) dimensions are no longer equivalent in anisotropic processes. It is worthwhile to note that the preceding results hold for the two dual codimension functions (i.e., for $c(\gamma)$, the codimension function of the singularities, as well as for $C(h)$, the codimension function of divergence of the statistics).

D.2. *Elliptical Dimensional Sampling*

The preceding results (especially equation (D8)) have immediate applications when analyzing data on different subspaces (e.g., planes, lines, etc.), since if we estimate the codimensions $C_{el}(h)$ (or $c_{el}(\gamma)$), using an inappropriate scale (such as an isotropic one), we will obtain apparent codimension functions $C_{a,F}$ (respectively, $c_{a,F}(\gamma)$) depending on the subspace (F) on which they are evaluated

$$C_{a,F}(h)/d_{a,el}(F) = C_{el}(h)/d_{el} \ (F) \qquad (D11)$$

$d_{a,el}(F)$ being the "apparent", or tested, (elliptical) dimension of the subspace F. For instance, we may evaluate the statification of the rain field by testing the following family of diagonal generators (where we have implicitly excluded differential rotations)

$$G_m = \begin{bmatrix} 1 & 0 & 0 \\ 0 & 1 & 0 \\ 0 & 0 & \mu_m \end{bmatrix} \qquad (D12)$$

Thus we have the following linear function of $\Delta\mu_m$ ($=\mu-\mu_m$), the difference between the vertical eigenvalue μ of the generator G of the process and the corresponding eigenvalue μ_m of the tested generators G_m):

$$f(\Delta\mu_m) = C_{m,3} - C_{m,2} = \Delta\mu_m \ C_{el}/d_{el} \qquad (D13)$$

with $C_{m,2}$ and $C_{m,3}$ corresponding to the apparent codimension functions of the process on the (two-dimensional horizontal) subspace and the whole (for isotropy, three-dimensional) space, as evaluated by a given generator G_m, C_{el} is the codimension function of the process (with corresponding elliptical dimension of the whole space d_{el}). Hence, equation (D13) leads to a linear estimator for $\Delta\mu_m$ obtained by averaging different estimates of either $C(h_j)$ or $c(\gamma_j)$ ($j=1,k$ over different empirical realizations).

REFERENCES:

Anselmet, F., Y. Gagne, E.J. Hopfinger, and R. A. Antonia, High order velocity structure functions in turbulent shear flows, *J. Fluid Mech.*, *140*, 63-75,1984.

Batchelor, G. I.,and A. A. Townshend, The nature of turbulent flow at large wavenumbers, *Proc. R. Soc. London, Ser. A 199*, 238-250,1949.

Bialas, A., and R. Peschanski, Moments of rapidity distributions as a measure of short-range fluctuations in high-energy collisions, *Nucl. Phys. B, B273*, 703-718, 1986.

Corrsin, S., On the Spectrum of Isotropic Temperature Fluctuations in an isotropic Turbulence, *J. Appl. Phys. 22*, 469-473 , 1951.

Frisch,U., and G. Parisi, A multifractal model of intermittency, in *Turbulence and Predictability in Geophysical Fluid Dynamics and Climate Dynamics*, edited by M. Ghil, R. Benzi, and G. Parisi, pp. 84-88, Elsevier North-Holland, New York, 1985.

Frisch, U., P. L. Sulem, and M. Nelkin, A simple dynamical model of intermittency in fully developed turbulence, *J. Fluid Mech., 87*, 719-724, 1978.

Gabriel, P., S. Lovejoy, G. L. Austin, and D. Schertzer, Radiative transfer in extremely variable fractal clouds, *Preprint of the 6th Conference on Atmospheric Radiation*, pp. 230-236, American Meteorological society, Boston, Mass.,1986.

Gabriel, P., S. Lovejoy, and D. Schertzer, Empirical determination of co-dimension functions for clouds and rain, *Scaling, fractals and non-linear variability in geophysics*, edited by D. Schertzer, and S. Lovejoy, Reidel, in press, 1987.

Gurvitch E., and M. Yaglom, Breakdown of eddies and probabilty distributions of small-scale turbulence, *Phys. Fluids, 16, Suppl. S*, S59-S65, 1967.

Halsey, T.C., M.H. Jensen, L.P. Kadanoff, I. Procaccia and B. I. Shraiman, Fractal measures and their singularities: the characterisation of strange sets, *Phys. Rev. A, 33*, 1141-1151, 1986.

Hentschel, H. G. E., and I. Proccacia, The infinite number of generalised dimensions of fractals and strange attractors, *Physica 8D*, 435-444,1983.

Herring, J.R., D. Schertzer, M. Lesieur, G.R. Newman, J.P. Chollet, and M. Larchevêque, A comparative assessment of sopectral closures as applied to passive scalar diffusion. *J. Fluid Mech., 124*, 411-420, 1982.

Kahane, J. P., Sur le Chaos Multiplicatif, *Ann. Sci. Math. Que., 9*, 435-444, 1985.

Kahane, J. P., Martingales and Random Measures, *Chinese Ann. Math.* , in press, 1987.

Kolmogorov, A. N., Local structure of turbulence in an incompressible liquid for very large Reynolds numbers. *Proc. Acad. Sci. USSR., Geochem. Sect.*, 30, 299-303,1949.

Ladoy, P., D. Schertzer, and S. Lovejoy, Une étude d'invariance locale-regionale des temperatures, *La Météorologie, 7*, 23-34, 1986.

Landau, L. D., and E. M. Lifshitz, *Fluid Mechanics*, Pergamon, New York, 1963.

Lavallée, D., D. Schertzer, and S. Lovejoy, On the determination of the co-dimension function ,*Scaling, fractals and non-linear variability in geophysics*, edited by D. Schertzer, and S. Lovejoy, Reidel, in press, 1987.

Leray, J., Sur le mouvement d'un liquide visqueux emplisent l'espace. *Acta Math., 63*, 193-248, 1934.

Levich, E., Helical fluctuations, fractal dimensions and path integrals in the theory of turbulence, *J. Fluid Mech.*, in press, 1987.

Levich E., and E. Tzvetkov, Helical inverse cascade in three-dimensional turbulence as a fundamental dominant mechanism in meso-scale atmospheric phenomena, *Phys. Rep., 128*, 1-37, 1985.

Levich, E., B. Levich, and A. Tsinober, Helical structures, fractal dimensions and renormalisation group approach in homogeneous turbulence, in *Turbulence and Chaotic Phenomena in Fluids*, pp. 309-317, edited by T. Tatsumi, Elsevier North-Holland, New York, 1984.

Lilly, D. K., Meso-scale variability of the atmosphere, *Mesoscale Meteorology– Theories, Observations and Models*, edited by D. K. Lilly and T. Gal'Chen, pp.13-24, D.Reidel, Hingham, Mass., 1983.

Lovejoy, S., Analysis of rain areas in terms of fractals, in *Preprints of the 20th conference on radar meteorology*, pp. 476-484, American Meteorological society, Boston, Mass.,1981.

Lovejoy, S., and B. Mandelbrot, Fractal properties of rain and a fractal model, *Tellus, 37A*, 209-232, 1985.

Lovejoy, S., and D. Schertzer, Buoyancy, shear, scaling and fractals, *Proceedings of 4th Conference on Atmospheric and Oceanic Waves and Stability*, pp. 102-108, American Meteorological Society, Boston, Mass. 1983.

Lovejoy, S., and D. Schertzer, Generalized scale invariance and fractal models of rain, Water Resour. Res., 21, 1233-1250,1985.

Lovejoy S., and D. Schertzer, Scale invariance, symmetries, fractals and stochastic simulations of atmospheric phenomena, *Bull. Am. Meteorol. Soc.,67*, 21-32, 1986a.

Lovejoy, S., and D. Schertzer, Scale invariance in climatological temperatures and the local spectral plateau. *Annales Geophysicae, 4B*, 401-410, 1986b.

Lovejoy, S., and D. Schertzer, Scale and dimension dependence in the detection and calibration of remotely sensed atmospheric phenomena, in *Preprints of the 2nd Conference on Satellite Meteorology and Remote Sensing and Applications*, pp. 176-182, American Meteorological society, Boston, Mass.,1986c.

Lovejoy, S., and D. Schertzer, Extreme variability, scaling and fractals in remote sensing: Analysis and simulation, in *Digital Image Processing in Remote Sensing*, edited by J. P. Muller, publish by Francis and Taylor, in press, 1987a.

Lovejoy, S., and D. Schertzer, Meeting report: Scaling, fractals and non-linear variability in geophysics. *EOS*, in press, 1987b.

Lovejoy S., D. Schertzer, and P. Ladoy, Fractal characterization of inhomogeneous measuring networks, *Nature, 319*, 43-44,1986a.

Lovejoy S., D. Schertzer, and P. Ladoy, Brighter outlook for weather forecasts, *Nature, 320*, 401-401, 1986b.

Lovejoy S., D. Schertzer, and A.A.Tsonis, Functional boxcounting and multiple elliptical dimensions in rain, *Science, 235*, 1036-1038, 1987.

Mandelbrot, B. Intermittent turbulence in self-similar cascades: Divergence of high moments and dimension of the carrier, *J. Fluid Mech., 62*, 331-350, 1974.

Mandelbrot, B., Intermittent turbulence and fractal dimension: Kurtosis and the spectral exponent 5/3+B, in *Turbulence and Navier-Stokes Equations*, edited by R. Teman, pp. 121-145, Springer-Verlag, New York,1976.

Mandelbrot, B., Self-affine fractal sets, I, the basic fractal dimensions, in *Fractals in Physics*, edited by L. Pietronero and E. Tosatti, pp. 3-15, Elsevier North-Holland, New York, 1986.

Mauldin R. D., and S. C. Williams, Random recursive constructions: Asymptotic geometric and topological properties, *Trans. Am. Math. Soc., 295*, 325-346, 1986.

Montariol, F., and R. Giraud, Engineer's Thesis, Météorologie Nationale, Toulouse, France, 1986.

Novikov, E. A., Intermittency and scale similarity of the structure of turbulent flow, *Prikl. Mat. Mekh., 35*, 266-277, 1970.

Novikov, E. A., and R. Stewart, Intermittency of turbulence and spectrum of fluctuations in energy-dissipation, *Izv. Akad. Nauk. SSSR, Ser. Geofiz, 3*, 408-412, 1964.

Novikov, E. A., High order correlations in a turbulent flow, *Izv. Akad. Nauk SSSR, Fiz. Atmos. Okeana, 1*, 788-796, 1965.

Novikov, E. A., Mathematical models of intermittency in turbulent flow, *Dokl. Akad. Nauk. SSSR, 168*, 1279-1282,1966.

Novikov, E. A., Scale similarity for random fields, *Dokl. Akad. Nauk SSSR, 184*, 1072-1075, 1969.

Obukhov, A., Structure of the Temperature Field is a Turbulent Flow, *Izv. Akad. Nauk. SSSR Ser. Geogr.J Jeofiz, 13*, 55-69,1949.

Pietronero, L., and A.P. Siebesma, Self-similarity of fluctuations in random multiplicative processes. *Phys. Rev. Lett., 57*, 1098-1101, 1986.

Richardson, L. F., Atmospheric diffusion shown on a distance neighbor graph. *Proc. R. Soc., London, Sec. A, 110*, 709-722, 1926.

Richardson, L. F. *Weather prediction by numerical process*, Cambridge U. Press, 1922, (Republished by Dover, New York,1965.)

Schertzer, D., and S. Lovejoy, The dimension of atmospheric motions, *Turbul. Chaotic Phenomena Fluids, IUTAM Symp., 1983*, 141-144, Kyoto U., Japan, 1983a.

Schertzer, D., and S. Lovejoy, Elliptical turbulence in the atmosphere, *Proceedings 4th Symposium on Turbulent Shear Flows*, pp.11.1-11.8, University of Karlsruhe,1983b.

Schertzer, D., and S. Lovejoy, On the dimension of atmospheric motions, *Turbulence and chaotic phenomena in fluids*, edited by T. Tatsumi, pp.505-508, Elsevier North-Holland, New York, 1984.

Schertzer, D., and S. Lovejoy, Generalized scale invariance in turbulent phenomena, *P.C.H. Journal, 6*, 623-635, 1985a.

Schertzer, D., and S. Lovejoy, The dimension and intermittency of atmospheric dynamics, *Turbulent Shear Flow, vol 4*, edited by B. Launder, pp. 7-33, Springer, New York, 1985b.

Schertzer, D., and S. Lovejoy, Generalized scale invariance in rotating and stratified turbulent flows, *Proceedings, 5th conference on Turbulent Shear Flows*, pp. 13.1-13.6, Cornell University, Ithica, N. Y. 1985c.

Schertzer, D., and S. Lovejoy, Singularités anisotropes, divergences des moments en turbulence: invariance d'echelle generalisée et processus multiplicatifs, *Ann. Sci. Math. Que.*, in press ,1987.

Schertzer, D., and S. Lovejoy, Generalized scale invariance and anisotropic intermittent fractals, in *Fractals in Physics*, edited by L. Pietronero, and E.Tosatti, Elsevier North-Holland, New York, 1986b.

Schertzer, D., and O. Simonin, A theoretical study of radiative cooling in homogeneous and isotropic turbulence, in *Turbulent Shear Flow, vol. 3*, edited by L. J. S. Bradbury, F. Durst, B. E. Launder, F. W. Schmidt, and J. H. Whitelaw, pp. 262-282, Springer, New York, 1983.

Visvanathan R., Fluctuations de suie et hiver nucléaire, Engineer's Thesis, Ecole Polytechnique, Paris, France, 1985.

Von Neumann, J., Recent theories in turbulence, *Collect. Works, 6*, 437-450, Pergamon, New York, 1963.

Waymire, E., Scaling limits and self-similarity in precipitation fields, *Water Resour. Res.,21*, 1251-1265, 1985.

Waymire, E., and V.K. Gupta, The mathematical structure of rainfall representations, parts 1-3, *Water Resour. Res., 17*, 1261-1294, 1981.

Waymire, E., and V.K. Gupta, On scaling and log-normality in rainfall?, *Scaling, fractals and non-linear variability in geophysics*, edited by, D. Schertzer, and S. Lovejoy, Reidel, in press, 1987.

Wilson J., S. Lovejoy, and D. Schertzer, Physically based cloud modeling by scaling multiplicative cascade processes, *Scaling, fractals and non-linear variability in geophysics*, edited by D. Schertzer, and S. Lovejoy, Reidel, in press, 1987.

Yaglom, A. M., The influence of the fluctuation in energy dissipation on the shape of turbulent characteristics in the inertial interval, *Sov. Phys. Dokl., 2*, 26-30, 1966.

S. Lovejoy, Departement of Physics, McGill University, 3600 University Street, Montréal, Québec, Canada H3A 2T8.

D. Schertzer, Etablissement d'Etudes et de Recherches Météorologiques, Centre de Recherches en Météorologie Dynamique, Météorologie Nationale, 2 avenue Rapp, 75007 Paris, France.